

Quantitative PAT with simplified P_N approximation

Hongkai Zhao*

Yimin Zhong†

Abstract

The photoacoustic tomography (PAT) is a hybrid modality that combines the optics and acoustics to obtain high resolution and high contrast imaging of heterogeneous media. In this work, our objective is to study the inverse problem in the quantitative step of PAT which aims to reconstruct the optical coefficients of the governing radiative transport equation from the ultrasound measurements. In our analysis, we take the simplified P_N approximation of the radiative transport equation as the physical model and then show the uniqueness and stability for this modified inverse problem. Numerical simulations based on synthetic data are presented to validate our analysis.

Key words. photoacoustic tomography (PAT), radiative transport equation, simplified P_N method, diffusion approximation, numerical reconstruction

1 Introduction

The photoacoustic tomography (PAT) [3, 6, 9, 19, 30, 26] is an emerging hybrid imaging modality that reconstructs high resolution images of optical properties of heterogeneous media. The PAT experiment uses a pulse of near-infra-red (NIR) laser into the medium of interest (e.g. fat, bone, tumor tissues). These photons propagate inside the medium by following the radiative transport process. During the propagation, a portion of the photons is absorbed by the medium and then converted into heat which causes a local thermoelastic expansion. Such expansion induces a transient pressure change and leads to the propagation of ultrasound. The ultrasound signals are measured around the boundary of the medium and we need to infer the optical properties from the acoustic measurements.

The photon transport process is usually modeled by radiative transport equation. Let $X = \Omega \times \mathbb{S}^2$, where Ω is the physical domain and \mathbb{S}^2 denotes the unit sphere in 3D, the photon density function $u(\mathbf{x}, \mathbf{v})$ satisfies the following

$$\begin{aligned} \mathbf{v} \cdot \nabla u(\mathbf{x}, \mathbf{v}) + \sigma_t(\mathbf{x})u(\mathbf{x}, \mathbf{v}) &= \sigma_s(\mathbf{x}) \int_{\mathbb{S}^2} p(\mathbf{v} \cdot \mathbf{v}')u(\mathbf{x}, \mathbf{v}')d\mathbf{v}' && \text{in } X, \\ u(\mathbf{x}, \mathbf{v}) &= f(\mathbf{x}, \mathbf{v}) && \text{on } \Gamma_-, \end{aligned} \quad (1)$$

where $\Gamma_- = \{(\mathbf{x}, \mathbf{v}) \in \partial\Omega \times \mathbb{S}^{d-1} \mid -\boldsymbol{\nu}(\mathbf{x}) \cdot \mathbf{v} > 0\}$ is the incoming boundary set. σ_s, σ_t are the scattering and total absorption coefficients respectively, $\sigma_a := \sigma_t - \sigma_s$ is the intrinsic absorption

*Department of Mathematics, Duke University, NC 27705, zhao@math.duke.edu .

†Department of Mathematics, Duke University, NC 27705, yimin.zhong@duke.edu .

coefficient. $f(\mathbf{x}, \mathbf{v})$ is the external illumination source. The scattering phase function $p(\mathbf{v} \cdot \mathbf{v}')$ is usually chosen as the Henyey-Greenstein function

$$p(\cos \theta) = \frac{1}{4\pi} \frac{1 - g^2}{(1 + g^2 - 2g \cos \theta)^{3/2}}, \quad (2)$$

where $g \in (-1, 1)$ is the anisotropy parameter.

The energy absorbed by the medium is $\sigma_a \int_{\mathbb{S}^2} u(\mathbf{x}, \mathbf{v}) d\mathbf{v}$, then the initial pressure field generated by the *photoacoustic effect* is:

$$H(\mathbf{x}) := \Upsilon(\mathbf{x}) \sigma_a(\mathbf{x}) \int_{\mathbb{S}^2} u(\mathbf{x}, \mathbf{v}) d\mathbf{v}, \quad (3)$$

where $\Upsilon(\mathbf{x})$ is the dimensionless Grüneisen coefficient which measures the efficiency of the photoacoustic effect.

Then the initial pressure field $H(\mathbf{x})$ propagates the ultrasound wave, which satisfies the following equation [27]:

$$\begin{aligned} \frac{1}{c^2(\mathbf{x})} \frac{\partial^2 p(\mathbf{x}, t)}{\partial t^2} - \Delta_{\mathbf{x}} p(\mathbf{x}, t) &= 0, & \text{in } \mathbb{R}^3 \times [0, \infty), \\ p(\mathbf{x}, 0) = H(\mathbf{x}), \quad \frac{\partial p}{\partial t}(\mathbf{x}, 0) &= 0, & \text{in } \mathbb{R}^3. \end{aligned} \quad (4)$$

Here $c(\mathbf{x})$ is the wave speed of the underlying medium. The measured acoustic signals are $p(\mathbf{x}, t)$ on $\partial\Omega \times [0, T]$ for sufficient large observation time T .

The usual reconstruction of PAT is a two-step process. The first step is to reconstruct the initial pressure field $H(\mathbf{x})$ from the ultrasound measurements. This problem has been studied extensively by [1, 2, 27, 15, 16] and the references therein. Here we assume this step has been finished and recovered the initial pressure field $H(\mathbf{x})$ and we focus on the second step to reconstruct the optical properties $(\sigma_a, \sigma_s, \Upsilon)$ from the quantity $H(\mathbf{x})$. Under the diffusion approximation, this quantitative PAT (qPAT) problem has been well studied [10, 25, 4, 5]. However, with the radiative transport equation (1), the multi-source inverse problem theory has not been well established except for *albedo* type data [20, 4], which requires infinitely many angularly resolved illumination sources $f(\mathbf{x}, \mathbf{v})$. It is still unclear about the uniqueness and stability of the reconstructions with finite many source functions or angularly independent sources.

In this paper, we aim to study the qPAT problem with the simplified P_N approximation to the equation (1) with angularly independent source functions, that is, $f(\mathbf{x}, \mathbf{v}) = f(\mathbf{x})$. The simplified P_N approximation is also referred as SP_N method, which is utilized to solve the radiative transport equation by forming a system of elliptic equations [22, 18]. The SP_N approximation with relatively small $N \leq 7$ has been applied to many optical imaging methods [31, 8, 17] and outperforms the traditional diffusion approximation (P_1 method). Theoretically, the simplified P_N approximation is derived from the P_N formulation [13] and the P_N approximation converges to the exact solution of RTE as $N \rightarrow \infty$. Under appropriate conditions SP_N and P_N are equivalent, see [22], however in general, they are different and not necessarily converging to the same limit. For the qPAT problem, the case with $N = 3$ has been considered in [11], in our work, we extend the theory to arbitrary order N under a unified framework.

Under the SP_N approximation, the RTE's solution is expanded with Legendre polynomials, which derives a weakly coupled diffusion equation system [18]. Formally, the 3D SP_N approximation takes the 1D P_N equations and replace the diffusion operators with 3D's counterpart, which

is

$$\begin{aligned}
& - \left(\frac{n+1}{2n+1} \right) \nabla \frac{1}{\sigma_{n+1}} \nabla \left[\left(\frac{n+2}{2n+3} \right) \phi_{n+2} + \left(\frac{n+1}{2n+3} \right) \phi_n \right] \\
& - \left(\frac{n}{2n+1} \right) \nabla \frac{1}{\sigma_{n-1}} \nabla \left[\left(\frac{n}{2n-1} \right) \phi_n + \left(\frac{n-1}{2n-1} \right) \phi_{n-2} \right] + \sigma_n \phi_n = 0
\end{aligned} \tag{5}$$

for $n = 2, 4, \dots, N-1$, where coefficients $\sigma_n = \sigma_a + \sigma_s(1-g^n)$, $\sigma_0 = \sigma_a$. Physically speaking, ϕ_n represents the n -th Legendre moments of the solution $u(\mathbf{x}, \mathbf{v})$ and ϕ_0 will be the angular average of the solution. The corresponding mixed boundary conditions are derived from the 1D P_N equation's boundary conditions by replacing $\frac{d}{dx}$ with $\mathbf{n} \cdot \nabla$ on the boundary [18].

In the following context, we let

$$\varphi_n = (2n-1)\phi_{2n-2} + (2n)\phi_{2n}, \quad n = 1, 2, \dots, (N+1)/2, \tag{6}$$

and the column vector $\Phi = [\varphi_1, \varphi_2, \dots, \varphi_{(N+1)/2}]^T$, which satisfies

$$\Phi = \begin{pmatrix} \varphi_1 \\ \varphi_2 \\ \varphi_3 \\ \vdots \\ \varphi_{(N+1)/2} \end{pmatrix} = M \begin{pmatrix} \phi_0 \\ \phi_2 \\ \phi_4 \\ \vdots \\ \phi_{N-1} \end{pmatrix} \quad \text{where } M := \begin{pmatrix} 1 & 2 & 0 & \dots & 0 \\ 0 & 3 & 4 & \dots & 0 \\ 0 & 0 & 5 & \dots & 0 \\ \vdots & \vdots & \vdots & \ddots & \vdots \\ 0 & 0 & 0 & \dots & N \end{pmatrix}, \tag{7}$$

since the matrix M is upper triangular, its inverse is also upper triangular, let the row vector $\mathbf{s}_k = [s_{k,1}, \dots, s_{k,(N+1)/2}]$ represent the k -th row of the inverse matrix M^{-1} , according to Lemma A.1, its entries are

$$s_{k,l} = \begin{cases} \frac{1}{2^{k-1}} (-1)^{l-k} \frac{((2l-2))! (2k-1)!}{(2l-1)! (2k-2)!}, & l \geq k, \\ 0, & \text{otherwise.} \end{cases} \tag{8}$$

Then we derive the SP_N diffusion system

$$-\nabla \cdot \frac{A_n}{(4n-1)\sigma_{2n-1}} \nabla \varphi_n - \nabla \cdot \frac{B_n}{(4n-5)\sigma_{2n-3}} \nabla \varphi_{n-1} + \sigma_{2n-2} \mathbf{s}_n \cdot \Phi = 0 \tag{9}$$

for $n = 1, 2, \dots, (N+1)/2$, where the constants A_n, B_n are defined by

$$A_n = \frac{2n-1}{(4n-3)}, \quad B_n = \frac{2n-2}{(4n-3)}.$$

We remark that the following matrix differs from M^T by only a factor of diagonal matrix,

$$\begin{pmatrix} A_1 & 0 & 0 & \dots & 0 \\ B_2 & A_2 & 0 & \dots & 0 \\ 0 & B_3 & A_3 & \dots & 0 \\ \vdots & \vdots & \ddots & \ddots & \vdots \\ 0 & 0 & 0 & B_{(N+1)/2} & A_{(N+1)/2} \end{pmatrix} = LM^T \quad \text{where } L := \begin{pmatrix} 1 & 0 & 0 & \dots & 0 \\ 0 & \frac{1}{5} & 0 & \dots & 0 \\ 0 & 0 & \frac{1}{9} & \dots & 0 \\ \vdots & \vdots & \ddots & \ddots & \vdots \\ 0 & 0 & 0 & 0 & \frac{1}{2N-1} \end{pmatrix}. \tag{10}$$

The corresponding mixed boundary conditions are

$$\sum_{n=1}^{(N+1)/2} \mu_{2m-1, 2n-2} \phi_{2n-2} + \frac{1}{(4m-1)\sigma_{2m-1}} \frac{\partial \varphi_m}{\partial \mathbf{n}} = k_{2m-1} f, \quad m = 1, 2, \dots, (N+1)/2. \tag{11}$$

The constants $\mu_{2m-1,2n-2}$ and k_{2m-1} are

$$\begin{aligned}\mu_{2m-1,2n-2} &= (4n-3) \int_0^1 P_{2m-1}(x)P_{2n-2}(x)dx \\ &= (-1)^{m+n-1} \frac{\Gamma(m+\frac{1}{2})\Gamma(n-\frac{1}{2})}{\pi\Gamma(m)\Gamma(n)(m+n-1)} \frac{(4n-3)}{2n-2m-1}, \\ k_{2m-1} &= (-1)^{m-1} \frac{(2m-1)!!}{(2m-1)(2m)(2m-2)!!}.\end{aligned}$$

For convenience, we also define the following matrices Σ_e and R for later uses,

$$\Sigma_e = \begin{pmatrix} \sigma_0 & 0 & 0 & \dots & 0 \\ 0 & \sigma_2 & 0 & \dots & 0 \\ 0 & 0 & \sigma_4 & \dots & 0 \\ \vdots & \vdots & \vdots & \ddots & \vdots \\ 0 & 0 & 0 & \dots & \sigma_{N-1} \end{pmatrix}$$

and

$$R = (R_{ij})_{i,j=1,2,\dots,(N+1)/2}, \quad \text{with } R_{ij} = \mu_{2i-1,2j-2}.$$

In the quantitative photoacoustic tomography, we suppose the datum $H(\mathbf{x}) = \Upsilon(\mathbf{x})\sigma_a(\mathbf{x})\phi_0(\mathbf{x})$ has been reconstructed from the measured acoustic signals. In the following sections, we will analyze the uniqueness and stability of reconstruction of the coefficients $\Upsilon, \sigma_a, \sigma_s$ from the internal data H . We also make the following general assumptions for the rest of paper.

\mathcal{A} -i The physical domain Ω is simply connected with $C^{2,1}$ boundary.

\mathcal{A} -ii The coefficients $(\sigma_a, \sigma_s, \Upsilon)$ are non-negative and bounded. There exists constants \underline{c} and \bar{c} that

$$0 \leq \underline{c} \leq \sigma_a, \sigma_s, \Upsilon \leq \bar{c} < \infty. \quad (12)$$

\mathcal{A} -iii The coefficient $\sigma_a, \sigma_s \in C^{1,1}(\bar{\Omega})$. There exists a constant M that

$$\|\sigma_a\|_{C^{1,1}(\Omega)}, \|\sigma_s\|_{C^{1,1}(\Omega)} \leq M < \infty.$$

Moreover, σ_a, σ_s are both known on $\partial\Omega$.

\mathcal{A} -iv The boundary source function $f \in H^{5/2}(\partial\Omega)$.

The rest of the paper is organized as follows. We first present in Section 2 some general properties of the forward problem with SP_N approximation. Then in Section 3 we consider the reconstruction of a single coefficient from a single data set $H(\mathbf{x})$ and the reconstruction of two coefficients simultaneously with multiple data in linearized settings. We then demonstrate some numerical simulations based on synthetic data in Section 4 to validate some of our theoretical results. Conclusions are found in Section 5.

2 General properties

For the forward problem, we establish the wellposedness for the SP_N approximation. In order to show there exists a unique weak solution $\Phi \in [H^1(\Omega)]^{(N+1)/2}$ for (9) and (11), we only have to consider the corresponding variational form for the diffusion system. Let $\Psi = [\psi_1, \psi_2, \dots, \psi_{(N+1)/2}]^T \in [H^1(\Omega)]^{(N+1)/2}$ be a test function, then the weak form of the SP_N system is

$$\begin{aligned} B(\Phi, \Psi) &:= \sum_{n=1}^{(N+1)/2} \int_{\Omega} \frac{1}{(4n-1)\sigma_{2n-1}} \nabla \varphi_n \cdot \nabla \psi_n d\mathbf{x} \\ &\quad + \int_{\Omega} \langle M^{-T} L^{-1} \Sigma_e M^{-1} \Phi, \Psi \rangle d\mathbf{x} + \int_{\partial\Omega} \langle R M^{-1} \Phi, \Psi \rangle ds \\ &= \mathcal{L}(f, \Psi), \end{aligned} \tag{13}$$

where $B(\cdot, \cdot)$ is a bilinear form, \mathcal{L} is a linear functional only involving boundary integrals that

$$\mathcal{L}(f, \Psi) := \sum_{n=1}^{(N+1)/2} k_{2n-1} \int_{\partial\Omega} f \psi_n ds. \tag{14}$$

We prove the following property of the bilinear form $B(\cdot, \cdot)$.

Theorem 2.1. *The bilinear form (13) is bounded and strictly coercive for any SP_N approximation.*

Proof. The boundedness is obvious since L , M are both invertible matrices. We only need to prove the coerciveness. In the following, we will show that the matrices $M \Sigma_e^{-1} L M^T$ and $M^T R$ are positive definite. For $M \Sigma_e^{-1} L M^T$, it is obvious since the diagonal matrix $\Sigma_e^{-1} L$ has all positive entries. For the matrix $M^T R$, we compute its (i, k) -th entry by

$$\begin{aligned} &(2i-1)R_{i,k} + (2i-2)R_{i-1,k} \\ &= (2i-1)(4k-3) \int_0^1 P_{2i-1}(x) P_{2k-2}(x) dx + (2i-2)(4k-3) \int_0^1 P_{2i-3}(x) P_{2k-2}(x) dx \\ &= (4i-3)(4k-3) \int_0^1 x P_{2i-2}(x) P_{2k-2}(x) dx \\ &= \int_0^1 q_i(x) q_k(x) dx \quad \text{with } q_i(x) = (4i-3)\sqrt{x} P_{2i-2}(x), \end{aligned} \tag{15}$$

where P_k is the k -th Legendre polynomial and we have used the recurrence relation

$$(2i-1)P_{2i-1}(x) + (2i-2)P_{2i-3}(x) = (4i-3)xP_{2i-2}(x). \tag{16}$$

Hence $M^T R$ is semi-positive definite. On the other hand, if there is a vector $\mathbf{z} = [z_1, \dots, z_{(N+1)/2}]^T \in \mathbb{R}^{(N+1)/2}$ that

$$0 = \mathbf{z}^T (M^T R) \mathbf{z} = \int_0^1 x \left(\sum_{k=1}^{(N+1)/2} z_k (4k-3) P_{2k-2}(x) \right)^2 dx, \tag{17}$$

then for any $x \in [0, 1]$, the following polynomial must vanish,

$$\sum_{k=1}^{(N+1)/2} z_k (4k-3) P_{2k-2}(x) = 0. \tag{18}$$

Hence the polynomial equals zero for any $x \in \mathbb{R}$ and use the fact $\{P_k(x)\}_{k=1}^{(N+1)/2}$ forms an orthogonal basis on $[-1, 1]$, then $\forall k, z_k = 0$. Therefore $M^T R$ is strictly positive definite, so is $RM^{-1} = M^{-T}(M^T R)M^{-1}$. \square

The wellposedness immediately derives from the Lax-Milgram theorem, there exists a unique weak solution $\Phi \in [H^1(\Omega)]^{(N+1)/2}$ for arbitrary odd integer N . In fact, using the assumptions \mathcal{A} -i to \mathcal{A} -iv, the regularity theorem of elliptic systems [23] implies that the unique solution $\Phi \in [H^3(\Omega)]^{(N+1)/2}$, by the Sobolev embedding, the solution $\Phi \in [C^{1,1/2}(\Omega)]^{(N+1)/2}$.

3 Reconstruction under SP_N approximation

Generally speaking, if σ_a is not negligible, the inverse problem is highly nonlinear and very challenging. Therefore in the following, we only consider the practical scenario that $\sigma_a \ll \sigma_s(1-g)$, which means we can simplify the coefficients $\sigma_n = \sigma_a + (1-g^n)\sigma_s \simeq (1-g^n)\sigma_s$ for $n \geq 1$ and $\sigma_0 = \sigma_a$. This simplification decouples the coefficients σ_a and σ_s . In particular, if $g = 0$, there is no need to perform such simplification.

Reconstruction of σ_a only. Suppose the coefficients Υ, σ_s are known on Ω , we consider the reconstruction of σ_a from a single measurement datum H . Using the assumption that $\sigma_n \simeq (1-g^n)\sigma_s$ for $n \geq 1$, the coefficients σ_n are all known for $n \geq 1$. Since $\sigma_a = \sigma_0$, then using $H(\mathbf{x}) = \Upsilon(\mathbf{x})\sigma_a(\mathbf{x})\phi_0(\mathbf{x})$ and $\phi_0 = \mathbf{s}_1 \cdot \Phi$, we derive that

$$\sigma_0(\mathbf{x}) = \frac{H(\mathbf{x})}{\Upsilon(\mathbf{x})\mathbf{s}_1 \cdot \Phi}. \quad (19)$$

By isolating the term relevant to σ_0 ($n = 0$) in the bilinear form (13), we can reformulated it as

$$\begin{aligned} B(\Phi, \Psi) &= \sum_{n=1}^{(N+1)/2} \int_{\Omega} \frac{1}{(4n-1)\sigma_{2n-1}} \nabla \varphi_n \cdot \nabla \psi_n d\mathbf{x} + \int_{\Omega} \frac{H(\mathbf{x})}{\Upsilon(\mathbf{x})\mathbf{s}_1 \cdot \Phi} (\mathbf{s}_1 \cdot \Phi)(\mathbf{s}_1 \cdot \Psi) d\mathbf{x} \\ &+ \sum_{n=2}^{(N+1)/2} \int_{\Omega} (4n-3)\sigma_{2n-2} (\mathbf{s}_n \cdot \Phi)(\mathbf{s}_n \cdot \Psi) d\mathbf{x} \\ &+ \int_{\partial\Omega} \langle RM^{-1}\Phi, \Psi \rangle ds. \end{aligned} \quad (20)$$

where the row vector \mathbf{s}_k denotes the k -th row of M^{-1} . We can establish the following uniqueness and stability result.

Theorem 3.1. *Given any SP_N approximation, under the assumptions \mathcal{A} -i to \mathcal{A} -iv and suppose (Υ, σ_s) are known, $\sigma_{a,1}$ and $\sigma_{a,2}$ are two admissible absorption coefficients, H_1, H_2 are the corresponding internal data, respectively. Then $H_1 = H_2$ implies $\sigma_{a,1} = \sigma_{a,2}$ and the following stability estimate holds*

$$\|(\sigma_{a,1} - \sigma_{a,2}) \frac{H_1}{\sigma_{a,1}\Upsilon}\|_{L^2(\Omega)} \leq C \|(H_1 - H_2)/\Upsilon\|_{L^2(\Omega)}, \quad (21)$$

where $C = C(N, \Omega)$ is a positive constant depending on N and Ω only.

Proof. Let Φ and $\tilde{\Phi}$ be the weak solutions to the SP_N system for the absorption coefficients $\sigma_{a,1}$ and $\sigma_{a,2}$, respectively. Let $\delta\Phi := \Phi - \tilde{\Phi} = [\delta\varphi_1, \dots, \delta\varphi_{(N+1)/2}]^T$, then from the bilinear form (20), we obtain the equation

$$\tilde{B}(\delta\Phi, \Psi) = - \int_{\Omega} \frac{H_1 - H_2}{\Upsilon} (\mathbf{s}_1 \cdot \Psi) d\mathbf{x}, \quad (22)$$

where the above modified bilinear form $\tilde{B}(\cdot, \cdot)$ is

$$\begin{aligned}\tilde{B}(\delta\Phi, \Psi) &= \sum_{n=1}^{(N+1)/2} \int_{\Omega} \frac{1}{(4n-1)\sigma_{2n-1}} \nabla \delta\varphi_n \cdot \nabla \psi_n d\mathbf{x} \\ &+ \sum_{n=2}^{(N+1)/2} \int_{\Omega} (4n-3)\sigma_{2n-2}(\mathbf{s}_n \cdot \delta\Phi)(\mathbf{s}_n \cdot \Psi) d\mathbf{x} \\ &+ \int_{\partial\Omega} \langle RM^{-1}\delta\Phi, \Psi \rangle ds.\end{aligned}\tag{23}$$

Since RM^{-1} is strictly positive definite, the coerciveness of $\tilde{B}(\cdot, \cdot)$ is immediately deduced from the Poincaré-Sobolev inequality [32] that $\forall u \in H^1(\Omega)$, $\Omega \subset \mathbb{R}^3$,

$$\|u\|_{L^6(\Omega)} \leq C_{ps} (\|\nabla u\|_{L^2(\Omega)} + \|u\|_{L^1(\partial\Omega)}),\tag{24}$$

where $C_{ps} = C_{ps}(\Omega)$ is a positive constant depending on Ω only. Therefore there exists another constant $C_1(N, \Omega)$ that

$$\begin{aligned}C_1(N, \Omega) \|\delta\Phi\|_{[L^2(\Omega)]^{(N+1)/2}}^2 &\leq \tilde{B}(\delta\Phi, \delta\Phi) = - \int_{\Omega} \frac{H_1 - H_2}{\Upsilon} (\mathbf{s}_1 \cdot \delta\Phi) d\mathbf{x} \\ &\leq \|(H_1 - H_2)/\Upsilon\|_{L^2(\Omega)} \|\mathbf{s}_1 \cdot \delta\Phi\|_{L^2(\Omega)} \\ &\leq \|(H_1 - H_2)/\Upsilon\|_{L^2(\Omega)} \|\mathbf{s}_1\|_{\ell^2} \|\delta\Phi\|_{[L^2(\Omega)]^{(N+1)/2}}\end{aligned}\tag{25}$$

by the Hölder inequality that

$$\|\mathbf{v} \cdot \Phi\|_{W^{k,p}(\Omega)} \leq \|\mathbf{v}\|_{\ell^q} \|\Phi\|_{[W^{k,p}(\Omega)]^{(N+1)/2}}, \quad \frac{1}{p} + \frac{1}{q} = 1,$$

where the norm $\|\cdot\|_{[W^{k,p}(\Omega)]^{(N+1)/2}}$ is defined by

$$\|\mathbf{f}\|_{[W^{k,p}(\Omega)]^{(N+1)/2}}^p = \sum_{n=1}^{(N+1)/2} \|f_n\|_{W^{k,p}(\Omega)}^p, \quad \mathbf{f} = [f_1, \dots, f_{(N+1)/2}]^T.$$

The estimate (25) implies

$$\|\delta\Phi\|_{[L^2(\Omega)]^{(N+1)/2}} \leq \frac{1}{C_1(N, \Omega)} \|(H_1 - H_2)/\Upsilon\|_{L^2(\Omega)} \|\mathbf{s}_1\|_{\ell^2}.\tag{26}$$

Therefore the uniqueness is proved. For the stability estimate, we compute

$$\begin{aligned}\frac{H_1 - H_2}{\Upsilon} &= \sigma_{a,1}(\mathbf{s}_1 \cdot \Phi) - \sigma_{a,2}(\mathbf{s}_1 \cdot \tilde{\Phi}) \\ &= (\sigma_{a,1} - \sigma_{a,2})(\mathbf{s}_1 \cdot \Phi) + \sigma_{a,2}(\mathbf{s}_1 \cdot \delta\Phi).\end{aligned}\tag{27}$$

Thus using (26), we obtain

$$\begin{aligned}\|(\sigma_{a,1} - \sigma_{a,2})(\mathbf{s}_1 \cdot \Phi)\|_{L^2(\Omega)} &\leq \left\| \frac{H_1 - H_2}{\Upsilon} \right\|_{L^2(\Omega)} + \|\sigma_{a,2}(\mathbf{s}_1 \cdot \delta\Phi)\|_{L^2(\Omega)} \\ &\leq \left(1 + \frac{\bar{c}\|\mathbf{s}_1\|_{\ell^2}^2}{C_1(N, \Omega)} \right) \left\| \frac{H_1 - H_2}{\Upsilon} \right\|_{L^2(\Omega)}.\end{aligned}\tag{28}$$

Our proof is completed by noticing (19). \square

The reconstruction algorithm for σ_a is then naturally divided into two steps. First, we solve Φ from the modified bilinear form (20), then recover σ_a by the relation (19) whenever $\mathbf{s}_1 \cdot \Phi \neq 0$. For the general SP_N system, we cannot guarantee the positivity of $\phi_0 = \mathbf{s}_1 \cdot \Phi$ for any positive source function $f(\mathbf{x})$.

Under appropriate conditions [22], the SP_N approximation will be eventually converging to the radiative transfer model. However, intuitively, when the order of system N grows, the reconstruction of the coefficients will be less stable due to the coupling of the Legendre moments in the solution. In the following, we study the relation of reconstruction's stability and the system order N . It can be shown that the reconstruction's stability estimate's constant in Theorem 3.1 grows at most proportional to $N^{11/8}(1 + \log N)$.

Corollary 3.2. *Under the assumptions A-i to A-iv, suppose (Υ, σ_s) are known, $\sigma_{a,1}, \sigma_{a,2}$ are two admissible absorption coefficients, H_1, H_2 are the corresponding internal data, respectively. Then $H_1 = H_2$ implies $\sigma_{a,1} = \sigma_{a,2}$ and the following stability estimate holds*

$$\|(\sigma_{a,1} - \sigma_{a,2}) \frac{H_1}{\sigma_{a,1} \Upsilon}\|_{L^2(\Omega)} \leq CN^{11/8}(1 + \log N) \|(H_1 - H_2)/\Upsilon\|_{L^2(\Omega)}, \quad (29)$$

where $C = C(\Omega)$ is a positive constant independent of N .

Proof. Recall the estimate (28), we only have to give an estimate for $C_1(N, \Omega)$ and $\|\mathbf{s}_1\|_{\ell^2}^2$ with respect to N . Using the equation (23), we can estimate the lower bound of the coerciveness for $\tilde{B}(\cdot, \cdot)$ by neglecting the second term,

$$\tilde{B}(\delta\Phi, \delta\Phi) \geq \frac{1}{(2N+1)\sigma_s} \|\nabla \delta\Phi\|_{[L^2(\Omega)]^{(N+1)/2}}^2 + \lambda_{(N+1)/2}(RM^{-1}) \|\delta\Phi\|_{[L^2(\partial\Omega)]^{(N+1)/2}}^2, \quad (30)$$

where $\lambda_n(K)$ denotes the n -th singular value of K ordered from largest to smallest. Use the inequality introduced in [21], we estimate the smallest singular value of RM^{-1} that

$$\lambda_{(N+1)/2}(RM^{-1}) \geq \lambda_{(N+1)/2}(R) \lambda_{(N+1)/2}(M^{-1}) = \lambda_{(N+1)/2}(R) / \lambda_1(M). \quad (31)$$

Since the largest singular value $\lambda_1(M) = \|M\|_{op}$, let $\mathbf{v} = [v_1, v_2, \dots, v_{(N+1)/2}]^T \in \mathbb{R}^{(N+1)/2}$ and take the convention that $v_{(N+3)/2} = 0$, then use the Cauchy-Schwartz inequality, we obtain

$$\|M\|_{op}^2 = \sup_{\|\mathbf{v}\|=1} \|M\mathbf{v}\|^2 = \sup_{\|\mathbf{v}\|=1} \sum_{k=1}^{(N+1)/2} ((2k-1)v_k + (2k)v_{k+1})^2 \leq 2N^2 \|\mathbf{v}\|^2 = 2N^2. \quad (32)$$

Therefore we have $\lambda_1(M) \leq \sqrt{2}N$. In the next, we only need to estimate the smallest singular value of R . According to the lower bound estimates introduced in [24, 14], the smallest singular value satisfies

$$\lambda_{(N+1)/2}(R) \geq \left(\frac{\frac{N-1}{2}}{\|R\|_F^2} \right)^{\frac{N-1}{4}} |\det(R)|, \quad (33)$$

where $\|\cdot\|_F$ denotes the Frobenius norm, then use the results from Lemma A.2 and Lemma A.3 in Appendix, we have the estimate

$$\lambda_{(N+1)/2}(R) \geq \left(\frac{N-1}{N+1} \right)^{\frac{N-1}{4}} |\det(R)| = \mathcal{O}(N^{-3/8}). \quad (34)$$

Therefore $C_1(N, \Omega) \geq c \min(\frac{1}{(2N+1)\sigma_s}, \lambda_{(N+1)/2}(RM^{-1})) = \mathcal{O}(N^{-11/8})$. To estimate the upper bound of $\|\mathbf{s}_1\|^2$, we compute the row vector $\mathbf{s}_1 = [s_{1,1}, \dots, s_{1,(N+1)/2}]$ by performing Gauss elimination on M and obtain

$$|s_{1,k}| = \frac{(2k-2)!!}{(2k-1)!!} = \frac{\sqrt{\pi}}{2} \frac{\Gamma(k)}{\Gamma(k + \frac{1}{2})}. \quad (35)$$

Use the Gautschi's inequality [12] that

$$\frac{1}{\sqrt{k + \frac{1}{2}}} < \frac{\Gamma(k)}{\Gamma(k + \frac{1}{2})} < \frac{1}{\sqrt{k - \frac{1}{2}}}, \quad (36)$$

we immediately find out

$$\|\mathbf{s}_1\|_{\ell^2}^2 \leq \frac{\pi}{4} \sum_{i=1}^{(N+1)/2} \frac{1}{i - \frac{1}{2}} = \mathcal{O}(1 + \log N). \quad (37)$$

From the result of Theorem 3.1, the stability estimate now can be formulated as

$$\|(\sigma_{a,1} - \sigma_{a,2})\mathbf{s}_1\Phi\|_{L^2(\Omega)} \leq \mathcal{O}(N^{11/8}(1 + \log N)) \left\| \frac{H_1 - H_2}{\Upsilon} \right\|_{L^2(\Omega)}. \quad (38)$$

□

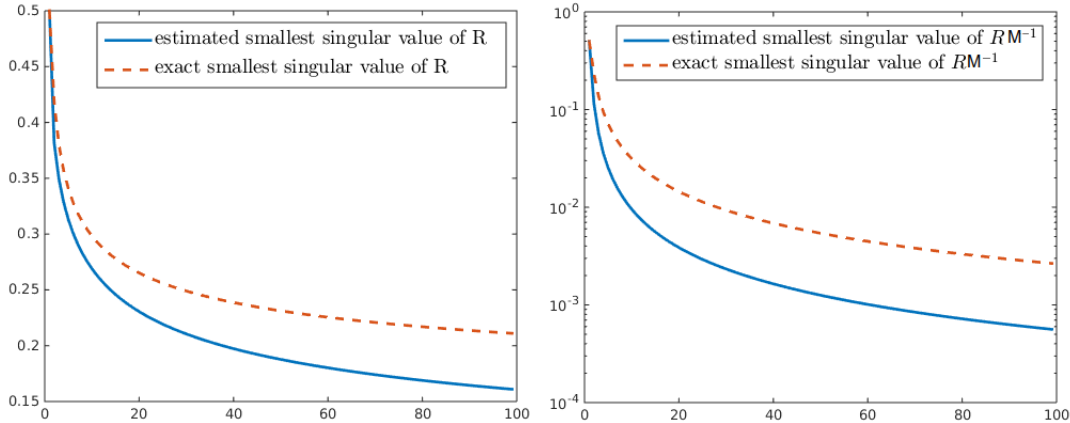


Figure 1: Decay of the smallest singular values with respect to the matrix sizes. The x -axis denotes the matrix size $(N + 1)/2$. Left: The red (dashed) line represents the exact smallest singular value of R and the blue (solid) line represents the estimated lower bound of the smallest singular value of R through (33). Right: The red (dashed) line represents the exact smallest singular value of RM^{-1} and the blue (solid) line represents the estimated lower bound of the smallest singular value of RM^{-1} through (31).

Remark 3.3. *It is possible to improve the above estimate by using a sharper bounded for the Frobenius norm $\|R\|_F$ in Lemma A.3. The simple bounds (31) and (33) are not sharp for the smallest singular value of R , see Fig 1. It seems possible to achieve better estimate through the calculation of R^{-1} 's Frobenius norm by following the technique in [29]. Use the Wielandt-Hoffman theorem, we can also deduce that R and the Cauchy-Toeplitz matrix with (i, j) -entry as $\frac{1/\pi}{i-j+\frac{1}{2}}$ share the equally distributed singular values, i.e., R 's singular values have a cluster at 1, see [28].*

Remark 3.4. As $N \rightarrow \infty$, the above result shows that the stability estimate's constant will also grow to infinity, this seems to give a negative answer to the uniqueness for qPAT with the radiative transport equation. However, such estimate is only meant for the worst case, since the boundary source could be chosen arbitrarily. In practice, if the source function f is sufficiently smooth, the datum with respect to the SP_N model $H = \Upsilon \sigma_a \mathbf{s}_1 \cdot \Phi$ will converge rapidly and the high order modes will decay sufficiently fast, which could counter the growth in the constant. This will be the future work.

Reconstruction of Υ only. Suppose the coefficients σ_a, σ_s are known and Υ is unknown, then the SP_N equation system is completely known and Φ could be uniquely solved, so we can reconstruct Υ explicitly by

$$\Upsilon = \frac{H(\mathbf{x})}{\sigma_0(\mathbf{x})(\mathbf{s}_1 \cdot \Phi)}. \quad (39)$$

The uniqueness and stability estimate will be straightforward, we conclude in the following theorem without proof.

Theorem 3.5. Under the assumptions \mathcal{A} -i to \mathcal{A} -iv, suppose (σ_a, σ_s) are known, Υ_1, Υ_2 are two Grüneisen coefficients, H_1, H_2 are the corresponding internal data, respectively. Then we have the following stability estimate

$$\|(\Upsilon_1 - \Upsilon_2) \frac{H_1}{\Upsilon_1}\|_{L^2(\Omega)} \leq C \|(H_1 - H_2)/\sigma_a\|_{L^2(\Omega)}, \quad (40)$$

the constant C does not depend on N .

Reconstruction of σ_s only. Suppose the coefficients Υ, σ_a are known and σ_s is unknown, then

$$\mathbf{s}_1 \cdot \Phi = \frac{H(\mathbf{x})}{\Upsilon(\mathbf{x})\sigma_0(\mathbf{x})} \quad (41)$$

is known from the measurement H . In addition, we also assume that σ_s is known on the boundary $\partial\Omega$. When $N = 1$, the reconstruction process of σ_s will be solving a linear transport equation [5] for σ_s^{-1} , while larger N will introduce extra nonlinearity from the coupling of solution components. The linearized case of SP_3 approximation has been recently studied in [11], which should be able to generalize to SP_N system with the similar technique. In the following, we assume $N \geq 3$, for the corresponding nonlinear inverse problem, let \mathbf{s}_k be the k -th row of M^{-1} and $\mathbf{u}_{k,n}$ be the n -th row of the rank-one matrix $\mathbf{s}_k^T \mathbf{s}_k$. We reformulate the equations from the bilinear form (13) as

$$-\nabla \cdot \left(\frac{1}{\sigma_s} \nabla \varphi_n \right) + \sigma_a \mathbf{p}_n \cdot \Phi + \sigma_s \mathbf{q}_n \cdot \Phi = 0, \quad n = 1, \dots, (N+1)/2, \quad (42)$$

where the row vectors \mathbf{p}_n and \mathbf{q}_n are defined by

$$\begin{aligned} \mathbf{p}_n &= (4n-1)(1-g^{2n-1})\mathbf{u}_{1,n}, \\ \mathbf{q}_n &= (4n-1)(1-g^{2n-1}) \sum_{k=2}^{(N+1)/2} (4k-3)(1-g^{2k-2})\mathbf{u}_{k,n}. \end{aligned} \quad (43)$$

For convenience, we also denote \mathbf{P} and \mathbf{Q} as the corresponding matrices with n -th rows as \mathbf{p}_n and \mathbf{q}_n , respectively. In the following, we first prove a simple lemma to estimate the variation in solutions with respect to changes in the scattering coefficient.

Lemma 3.6. *Under the assumptions \mathcal{A} -i to \mathcal{A} -iv, suppose $\sigma_{s,1}$ and $\sigma_{s,2}$ are two admissible scattering coefficients that $\delta\sigma_s = \sigma_{s,1} - \sigma_{s,2}$ satisfies $\delta\sigma_s = 0$ on $\partial\Omega$. Let $\Phi_i = [\varphi_{i,1}, \dots, \varphi_{i,(N+1)/2}]^T \in [H^1(\Omega)]^{(N+1)/2}$ the solution associated with scattering coefficient $\sigma_{s,i}$, $i = 1, 2$, then*

$$\|\Phi_1 - \Phi_2\|_{[H^1(\Omega)]^{(N+1)/2}} \leq C \frac{N^{23/8}}{3(1-g)} \|\Phi_1\|_{[W^{1,\infty}(\Omega)]^{(N+1)/2}} \|\sigma_{s,1} - \sigma_{s,2}\|_{L^2(\Omega)}, \quad (44)$$

where C is a positive constant independent of N .

Proof. Let $B_i(\cdot, \cdot)$ the bilinear form in (13) for coefficient pair $(\sigma_a, \sigma_{s,i})$, $i = 1, 2$, then for any test function $\Psi \in [H^1(\Omega)]^{(N+1)/2}$, we have

$$B_1(\Phi_1, \Psi) = B_2(\Phi_2, \Psi). \quad (45)$$

Denote $\delta\Phi = [\delta\varphi_1, \dots, \delta\varphi_{(N+1)/2}]^T := \Phi_1 - \Phi_2$, by Cauchy-Schwartz inequality, we have

$$\begin{aligned} B_2(\delta\Phi, \delta\Phi) &= \sum_{n=1}^{(N+1)/2} \int_{\Omega} \frac{1}{(4n-1)(1-g^{2n-1})} \left[\frac{\delta\sigma_s}{\sigma_{s,1}\sigma_{s,2}} \nabla\varphi_{1,n} \cdot \nabla\delta\varphi_n - \delta\sigma_s \mathbf{q}_n \cdot \Phi_1 \delta\varphi_n \right] d\mathbf{x} \\ &\leq \theta \sum_{n=1}^{(N+1)/2} \left[\|\nabla\delta\varphi_n\|_{L^2(\Omega)} \left\| \frac{\delta\sigma_s \nabla\varphi_{1,n}}{\sigma_{s,1}\sigma_{s,2}} \right\|_{L^2(\Omega)} + \frac{3\|\delta\varphi_n\|_{L^2(\Omega)}}{4n-1} \|\delta\sigma_s \mathbf{q}_n \cdot \Phi_1\|_{L^2(\Omega)} \right] \\ &\leq \theta \kappa \|\delta\sigma_s\|_{L^2(\Omega)} \sum_{n=1}^{(N+1)/2} \|\delta\varphi_n\|_{H^1(\Omega)} \\ &\leq \theta \kappa \sqrt{\frac{(N+1)}{2}} \|\delta\sigma_s\|_{L^2(\Omega)} \|\delta\Phi\|_{[H^1(\Omega)]^{(N+1)/2}}, \end{aligned} \quad (46)$$

where the constants $\theta = (3(1-g))^{-1}$, $\kappa = \sup_{n \geq 1} \|\nabla\varphi_{1,n}/(\sigma_{s,1}\sigma_{s,2})\|_{L^\infty(\Omega)} + \frac{3}{4n-1} \|\mathbf{q}_n \cdot \Phi_1\|_{L^\infty(\Omega)}$. Since $\sigma_{s,1}, \sigma_{s,2}$ are bounded from below by positive constants, the first term in κ is bounded by $\|\Phi_1\|_{[W^{1,\infty}]^{(N+1)/2}}$. The second term needs to estimate $\sup_{n \geq 1} \frac{3}{4n-1} \|\mathbf{q}_n\|_{\ell^1}$. From the definition of \mathbf{q}_n in (43), we can deduce that

$$\begin{aligned} \frac{1}{4n-1} \|\mathbf{q}_n\|_{\ell^1} &\leq \sum_{k=2}^{(N+1)/2} (4k-3) \|\mathbf{u}_{k,n}\|_{\ell^1} \\ &= \sum_{k=2}^n (4k-3) \sum_{j=k}^{(N+1)/2} |s_{k,n} s_{k,j}| \\ &< \sum_{k=2}^n \sum_{j=k}^{(N+1)/2} \frac{(k+\frac{1}{2})(4k-3)}{(2k-1)^2} \frac{1}{\sqrt{j-\frac{1}{2}}\sqrt{n-\frac{1}{2}}} \quad (\text{Gaustchi's inequality}) \\ &\leq \frac{1}{\sqrt{n-\frac{1}{2}}} \sum_{k=2}^n \sum_{j=k}^{(N+1)/2} \frac{2}{\sqrt{j-\frac{1}{2}}} \quad (\text{since } \frac{1}{2}(k+1)(4k-3) \leq (2k-1)^2) \\ &= \mathcal{O}(N). \end{aligned} \quad (47)$$

This implies $\kappa \leq cN \|\Phi_1\|_{[W^{1,\infty}(\Omega)]^{(N+1)/2}}$ for certain constant $c > 0$. On the other hand, from the Corollary 3.2, there exists a constant C_1 independent of N that

$$B_2(\delta\Phi, \delta\Phi) \geq C_1 N^{-11/8} \|\delta\Phi\|_{[H^1(\Omega)]^{(N+1)/2}}^2. \quad (48)$$

Combine the estimates (48) and (46), we obtain

$$\|\delta\Phi\|_{H^1(\Omega)} \leq \frac{\mathbf{c}}{C_1} \frac{N^{23/8}}{3(1-g)} \|\Phi_1\|_{[W^{1,\infty}(\Omega)]^{(N+1)/2}} \|\delta\sigma_s\|_{L^2}. \quad (49)$$

□

Theorem 3.7. *Under the assumptions A-i to A-iv, suppose (σ_a, Υ) are known, let $\sigma_{s,1}$ and $\sigma_{s,2}$ be two admissible scattering coefficients with $\sigma_{s,1} = \sigma_{s,2}$ on the boundary $\partial\Omega$. Let Φ_1 and Φ_2 the solutions to the SP_N system with scattering coefficients $\sigma_{s,1}$ and $\sigma_{s,2}$ respectively. H_1 and H_2 denote the corresponding internal data for $\sigma_{s,1}$ and $\sigma_{s,2}$ respectively. Then we have the following estimate*

$$\int_{\Omega} \mathcal{V}_N(\mathbf{x}; \lambda) \left(\frac{\sigma_{s,1} - \sigma_{s,2}}{\sigma_{s,2}} \right)^2 d\mathbf{x} \leq \frac{\mathbf{C}}{\lambda} N^2 \left\| \frac{H_1 - H_2}{\Upsilon\sigma_a} \right\|_{H^2(\Omega)}^2, \quad (50)$$

where $\lambda \in (0, 2\underline{c})$ is an arbitrary constant, $\mathcal{V}_N(\mathbf{x}; \lambda)$ is

$$\mathcal{V}_N(\mathbf{x}) := (\sigma_{s,1} + 2\underline{c} - \lambda)(\mathbf{s}_1 \cdot \mathbf{Q}\Phi_1)^2 + \kappa_N \frac{H_1}{\Upsilon} (\mathbf{s}_1 \cdot \mathbf{Q}\Phi_1) - \frac{1}{\sigma_{s,1}} \nabla \frac{H_1}{\Upsilon\sigma_a} \cdot \nabla (\mathbf{s}_1 \cdot \mathbf{Q}\Phi_1) - 2\underline{c}^2 \mathcal{Y}, \quad (51)$$

with

$$\begin{aligned} \mathcal{Y} &:= C_3 N^{39/8} \|\mathbf{s}_1 \cdot \mathbf{Q}\Phi_1\|_{L^\infty(\Omega)} \|\Phi_1\|_{W^{1,\infty}(\Omega)}, \\ \kappa_N &:= \sum_{n=1}^{(N+1)/2} (4n-1)(1-g^{2n-1}) s_{1,n}^2, \end{aligned} \quad (52)$$

the constants \mathbf{C}, C_3 are independent of N . When $\mathcal{V}_N(\mathbf{x}; \lambda) > 0, \forall \mathbf{x} \in \Omega$, then $H_1 = H_2$ a.e. on Ω implies $\sigma_{s,1} = \sigma_{s,2}$ a.e..

Proof. For $n = 1, \dots, (N+1)/2$, we have the following SP_N systems for Φ_1 and Φ_2 ,

$$\begin{aligned} -\nabla \cdot \left(\frac{1}{\sigma_{s,1}} \nabla \varphi_{1,n} \right) + \sigma_a \mathbf{p}_n \cdot \Phi_1 + \sigma_{s,1} \mathbf{q}_n \cdot \Phi_1 &= 0, \\ -\nabla \cdot \left(\frac{1}{\sigma_{s,2}} \nabla \varphi_{2,n} \right) + \sigma_a \mathbf{p}_n \cdot \Phi_2 + \sigma_{s,2} \mathbf{q}_n \cdot \Phi_2 &= 0, \end{aligned} \quad (53)$$

with the mixed boundary condition (11). Since Υ and σ_a are known, the measurements are given by

$$\mathbf{s}_1 \cdot \Phi_i = \frac{H_i}{\Upsilon\sigma_a}, \quad i = 1, 2. \quad (54)$$

Therefore multiply (53) with $s_{1,n}$ and take summation over n , we get

$$-\nabla \cdot \left(\frac{1}{\sigma_{s,i}} \nabla \frac{H_i}{\Upsilon\sigma_a} \right) + \mathbf{s}_1 \cdot (\sigma_a \mathbf{P}\Phi_i + \sigma_{s,i} \mathbf{Q}\Phi_i) = 0, \quad i = 1, 2. \quad (55)$$

Take the difference between equations (55) with $\sigma_{s,1}$ and $\sigma_{s,2}$, respectively. Let $\delta\sigma_s = \sigma_{s,1} - \sigma_{s,2}$, $\delta\Phi = \Phi_1 - \Phi_2$ and $\delta H = H_1 - H_2$, then

$$-\nabla \cdot \left(\frac{-\delta\sigma_s}{\sigma_{s,1}\sigma_{s,2}} \nabla \frac{H_1}{\Upsilon\sigma_a} \right) - \nabla \cdot \left(\frac{1}{\sigma_{s,2}} \nabla \frac{\delta H}{\Upsilon\sigma_a} \right) + \mathbf{s}_1 \cdot (\sigma_a \mathbf{P}\delta\Phi + \delta\sigma_s \mathbf{Q}\Phi_1 + \sigma_{s,2} \mathbf{Q}\delta\Phi) = 0. \quad (56)$$

Use the following identity,

$$\frac{\delta\sigma_s}{\sigma_{s,2}} \nabla \cdot \left(\frac{\delta\sigma_s}{\sigma_{s,2}} \frac{1}{\sigma_{s,1}} \nabla \frac{H_1}{\Upsilon\sigma_a} \right) = \frac{1}{2} \left(\frac{\delta\sigma_s}{\sigma_{s,2}} \right)^2 \nabla \cdot \left(\frac{1}{\sigma_{s,1}} \nabla \frac{H_1}{\Upsilon\sigma_a} \right) + \frac{1}{2} \nabla \cdot \left(\left(\frac{\delta\sigma_s}{\sigma_{s,2}} \right)^2 \frac{1}{\sigma_{s,1}} \nabla \frac{H_1}{\Upsilon\sigma_a} \right), \quad (57)$$

we multiply (56) with $\delta\sigma_s/\sigma_{s,2}$, then

$$\begin{aligned} & \frac{1}{2} \left(\frac{\delta\sigma_s}{\sigma_{s,2}} \right)^2 \nabla \cdot \left(\frac{1}{\sigma_{s,1}} \nabla \frac{H_1}{\Upsilon\sigma_a} \right) + \frac{1}{2} \nabla \cdot \left(\left(\frac{\delta\sigma_s}{\sigma_{s,2}} \right)^2 \frac{1}{\sigma_{s,1}} \nabla \frac{H_1}{\Upsilon\sigma_a} \right) \\ & - \frac{\delta\sigma_s}{\sigma_{s,2}} \nabla \cdot \left(\frac{1}{\sigma_{s,2}} \nabla \frac{\delta H}{\Upsilon\sigma_a} \right) + \frac{\delta\sigma_s}{\sigma_{s,2}} \mathbf{s}_1 \cdot (\sigma_a \mathbf{P} \delta\Phi + \delta\sigma_s \mathbf{Q} \Phi_1 + \sigma_{s,2} \mathbf{Q} \delta\Phi) = 0. \end{aligned} \quad (58)$$

The first term can be replaced from (55) that

$$\frac{1}{2} \left(\frac{\delta\sigma_s}{\sigma_{s,2}} \right)^2 \nabla \cdot \left(\frac{1}{\sigma_{s,1}} \nabla \frac{H_1}{\Upsilon\sigma_a} \right) = \frac{1}{2} \left(\frac{\delta\sigma_s}{\sigma_{s,2}} \right)^2 \mathbf{s}_1 \cdot (\sigma_a \mathbf{P} \Phi_1 + \sigma_{s,1} \mathbf{Q} \Phi_1), \quad (59)$$

then combine (58) and (59), multiply the test function $\psi = \mathbf{s}_1 \cdot \mathbf{Q} \Phi_1 \in H^1(\Omega)$ to (58) and integrate over Ω . Notice that $\delta\sigma_s = 0$ on $\partial\Omega$, we obtain

$$\begin{aligned} & \frac{1}{2} \int_{\Omega} \left(\frac{\delta\sigma_s}{\sigma_{s,2}} \right)^2 \left[\mathbf{s}_1 \cdot (\sigma_a \mathbf{P} + \sigma_{s,1} \mathbf{Q} + 2\sigma_{s,2} \mathbf{Q}) \Phi_1 (\mathbf{s}_1 \cdot \mathbf{Q} \Phi_1) - \frac{1}{\sigma_{s,1}} \nabla \frac{H_1}{\Upsilon\sigma_a} \cdot \nabla (\mathbf{s}_1 \cdot \mathbf{Q} \Phi_1) \right] d\mathbf{x} \\ & - \int_{\Omega} \frac{\delta\sigma_s}{\sigma_{s,2}} \left[\nabla \cdot \left(\frac{1}{\sigma_{s,2}} \nabla \frac{\delta H}{\Upsilon\sigma_a} \right) - \mathbf{s}_1 \cdot (\sigma_a \mathbf{P} \delta\Phi + \sigma_{s,2} \mathbf{Q} \delta\Phi) \right] (\mathbf{s}_1 \cdot \mathbf{Q} \Phi_1) d\mathbf{x} = 0. \end{aligned} \quad (60)$$

In the next, observe that

$$\mathbf{s}_1 \cdot \mathbf{P} = \sum_{n=1}^{(N+1)/2} (4n-1)(1-g^{2n-1}) s_{1,n} \mathbf{u}_{1,n} = \left(\sum_{n=1}^{(N+1)/2} (4n-1)(1-g^{2n-1}) s_{1,n}^2 \right) \mathbf{s}_1, \quad (61)$$

therefore in (60), we can replace

$$\begin{aligned} \sigma_a \mathbf{s}_1 \cdot \mathbf{P} \delta\Phi &= \left(\sum_{n=1}^{(N+1)/2} (4n-1)(1-g^{2n-1}) s_{1,n}^2 \right) \frac{\delta H}{\Upsilon}, \\ \sigma_a \mathbf{s}_1 \cdot \mathbf{P} \Phi_1 &= \left(\sum_{n=1}^{(N+1)/2} (4n-1)(1-g^{2n-1}) s_{1,n}^2 \right) \frac{H_1}{\Upsilon}. \end{aligned} \quad (62)$$

Define the constant $\kappa_N := \sum_{n=1}^{(N+1)/2} (4n-1)(1-g^{2n-1}) s_{1,n}^2$, since $|s_{1,n}|^2 = \Theta(n^{-1})$, then $\kappa_N = \Theta(N)$, the equation (60) can be further reduced to

$$\begin{aligned} & \frac{1}{2} \int_{\Omega} \left(\frac{\delta\sigma_s}{\sigma_{s,2}} \right)^2 \left[(\sigma_{s,1} + 2\sigma_{s,2}) (\mathbf{s}_1 \cdot \mathbf{Q} \Phi_1)^2 + \kappa_N \frac{H_1}{\Upsilon} (\mathbf{s}_1 \cdot \mathbf{Q} \Phi_1) - \frac{1}{\sigma_{s,1}} \nabla \frac{H_1}{\Upsilon\sigma_a} \cdot \nabla (\mathbf{s}_1 \cdot \mathbf{Q} \Phi_1) \right] d\mathbf{x} \\ & = \int_{\Omega} \frac{\delta\sigma_s}{\sigma_{s,2}} \left[\nabla \cdot \left(\frac{1}{\sigma_{s,2}} \nabla \frac{\delta H}{\Upsilon\sigma_a} \right) - \kappa_N \frac{\delta H}{\Upsilon} - \sigma_{s,2} (\mathbf{s}_1 \cdot \mathbf{Q} \delta\Phi) \right] (\mathbf{s}_1 \cdot \mathbf{Q} \Phi_1) d\mathbf{x}. \end{aligned} \quad (63)$$

Due to Lemma A.4, $\|\mathbf{s}_1 \cdot \mathbf{Q}\|_{\ell^p} \leq C_2 N^{3/2+1/p}$ for certain constant C_2 independent of N , then combine with Lemma 3.6, the second term on right-hand-side of (63) is bounded by

$$\begin{aligned} \left| \int_{\Omega} \delta\sigma_s (\mathbf{s}_1 \cdot \mathbf{Q}\delta\Phi) (\mathbf{s}_1 \cdot \mathbf{Q}\Phi_1) d\mathbf{x} \right| &\leq \|\mathbf{s}_1 \cdot \mathbf{Q}\|_{\ell^2} \|\delta\sigma_s\|_{L^2(\Omega)} \|\delta\Phi\|_{L^2(\Omega)} \|\mathbf{s}_1 \cdot \mathbf{Q}\Phi_1\|_{L^\infty(\Omega)} \\ &\leq C_2 N^2 \|\delta\sigma_s\|_{L^2(\Omega)} \|\delta\Phi\|_{L^2(\Omega)} \|\mathbf{s}_1 \cdot \mathbf{Q}\Phi_1\|_{L^\infty(\Omega)} \\ &\leq C_3 N^{39/8} \|\Phi_1\|_{W^{1,\infty}(\Omega)} \|\mathbf{s}_1 \cdot \mathbf{Q}\Phi_1\|_{L^\infty(\Omega)} \|\delta\sigma_s\|_{L^2(\Omega)}^2, \end{aligned}$$

where the constant C_3 is independent of N as well. Let \mathcal{X} and \mathcal{Y} denote the following quantities

$$\begin{aligned} \mathcal{X} &:= \kappa_N \frac{H_1}{\Upsilon} (\mathbf{s}_1 \cdot \mathbf{Q}\Phi_1) - \frac{1}{\sigma_{s,1}} \nabla \frac{H_1}{\Upsilon \sigma_a} \cdot \nabla (\mathbf{s}_1 \cdot \mathbf{Q}\Phi_1), \\ \mathcal{Y} &:= C_3 N^{39/8} \|\Phi_1\|_{W^{1,\infty}(\Omega)} \|\mathbf{s}_1 \cdot \mathbf{Q}\Phi_1\|_{L^\infty(\Omega)}, \end{aligned} \quad (64)$$

then we obtain the following inequality,

$$\begin{aligned} &\frac{1}{2} \int_{\Omega} \left(\frac{\delta\sigma_s}{\sigma_{s,2}} \right)^2 [(\sigma_{s,1} + 2\sigma_{s,2})(\mathbf{s}_1 \cdot \mathbf{Q}\Phi_1)^2 + \mathcal{X} - 2\sigma_{s,2}^2 \mathcal{Y}] d\mathbf{x} \\ &\leq \int_{\Omega} \frac{\delta\sigma_s}{\sigma_{s,2}} \left(\nabla \cdot \left(\frac{1}{\sigma_{s,2}} \nabla \frac{\delta H}{\Upsilon \sigma_a} \right) - \kappa_N \frac{\delta H}{\Upsilon} \right) (\mathbf{s}_1 \cdot \mathbf{Q}\Phi_1) d\mathbf{x} \\ &\leq \frac{\lambda}{2} \int_{\Omega} \left[\frac{\delta\sigma_s}{\sigma_{s,2}} (\mathbf{s}_1 \cdot \mathbf{Q}\Phi_1) \right]^2 d\mathbf{x} + \frac{1}{2\lambda} \int_{\Omega} \left(\nabla \cdot \left(\frac{1}{\sigma_{s,2}} \nabla \frac{\delta H}{\Upsilon \sigma_a} \right) - \kappa_N \frac{\delta H}{\Upsilon} \right)^2 d\mathbf{x}, \end{aligned} \quad (65)$$

where $\lambda > 0$ is an arbitrary number and the last inequality has used the AM-GM inequality. For the uniqueness, we let $\delta H = 0$ in above inequality, then it becomes

$$\int_{\Omega} \left(\frac{\delta\sigma_s}{\sigma_{s,2}} \right)^2 [(\sigma_{s,1} + 2\sigma_{s,2} - \lambda)(\mathbf{s}_1 \cdot \mathbf{Q}\Phi_1)^2 + \mathcal{X} - 2\sigma_{s,2}^2 \mathcal{Y}] d\mathbf{x} \leq 0. \quad (66)$$

Recall that $\underline{c} \leq \sigma_{s,2} \leq \bar{c}$, therefore if

$$(\sigma_{s,1} + 2\underline{c} - \lambda)(\mathbf{s}_1 \cdot \mathbf{Q}\Phi_1)^2 + \kappa_N \frac{H_1}{\Upsilon} (\mathbf{s}_1 \cdot \mathbf{Q}\Phi_1) - \frac{1}{\sigma_{s,1}} \nabla \frac{H_1}{\Upsilon \sigma_a} \cdot \nabla (\mathbf{s}_1 \cdot \mathbf{Q}\Phi_1) > 2\bar{c}^2 \mathcal{Y}, \quad (67)$$

we could conclude that $\delta\sigma_s = 0$ a.e.. The stability estimate is straightforward by noticing $\kappa_N = \mathcal{O}(N)$. \square

Remark 3.8. As $N \rightarrow \infty$, the requirement that $\mathcal{V}(x; \lambda) > 0$ could be difficult to fulfill since the growth of \mathcal{Y} is much faster than the other terms. The estimate could be greatly improved by giving a tighter bound to $\int_{\Omega} \delta\sigma_s (\mathbf{s}_1 \cdot \mathbf{Q}\delta\Phi) (\mathbf{s}_1 \cdot \mathbf{Q}\Phi_1) d\mathbf{x}$, for instance, estimate the Frechét derivative of $\frac{\delta\Phi}{\delta\sigma_s}$.

In the next, we focus on two important cases of simultaneous reconstructions: (Υ, σ_a) and (σ_a, σ_s) with multiple illumination sources. In SP_1 , one can only reconstruct any two coefficients with the knowledge about the third one [5, 25] and it is impossible to recover all of them unless additional information is provided. In SP_N , it is still unclear whether or not all of the coefficients can be recovered uniquely.

Reconstruction of σ_a and Υ . In this case, we consider the simultaneous reconstruction of both σ_a and Υ with multiple sources f_j , $1 \leq j \leq J$ ($J \geq 2$). We denote H_j the corresponding

measurement for f_j from qPAT. The simplest case SP_1 is studied in [5, 25] and linearized case of SP_3 is discussed in [11]. The key observation is that the ratio of two measurements is independent of the coefficients, which only implicitly depends on σ_a . We first consider the linearized setting, suppose the scattering coefficient σ_s and the background absorption and Grüneisen coefficients σ_a, Υ are known and the perturbations are $\delta\sigma_s, \delta\Upsilon$. For each $1 \leq j \leq J$, suppose Φ_j is the background solution with source f_j , the perturbation in the solution is denoted by $\delta\Phi_j$, then by linearizing (42), $\delta\Phi_j = [\delta\varphi_{j,1}, \dots, \delta\varphi_{(N+1)/2}]^T$ satisfies the linearized SP_N system

$$-\nabla \cdot \left(\frac{1}{\sigma_s} \nabla \delta\varphi_{j,n} \right) + \sigma_a \mathbf{p}_n \cdot \delta\Phi_j + \sigma_s \mathbf{q}_n \cdot \delta\Phi_j = -\delta\sigma_a \mathbf{p}_n \cdot \Phi_j, \quad n = 1, \dots, (N+1)/2. \quad (68)$$

For any pair of indices $1 \leq i < j \leq J$, we define the following quantity

$$\mathcal{H}_{ij} := (\mathbf{s}_1 \cdot \Phi_i) \frac{\delta H_j}{\sigma_a \Upsilon} - (\mathbf{s}_1 \cdot \Phi_j) \frac{\delta H_i}{\sigma_a \Upsilon} = (\mathbf{s}_1 \cdot \Phi_i)(\mathbf{s}_1 \cdot \delta\Phi_j) - (\mathbf{s}_1 \cdot \Phi_j)(\mathbf{s}_1 \cdot \delta\Phi_i), \quad (69)$$

which is known and only depends on $\delta\sigma_a$ and independent of Υ . Our reconstruction will be a natural two-step process, first solve $\delta\sigma_a$ from the crossing quantity \mathcal{H}_{ij} ($1 \leq i < j \leq J$), then solve $\delta\Phi_i$ using the recovered $\delta\sigma_a$, finally if $\sigma_a > 0$ find $\delta\Upsilon$ through

$$\delta\Upsilon = \frac{1}{J} \sum_{j=1}^J \frac{\delta H_j - \Upsilon \sigma_a \mathbf{s}_1 \cdot \delta\Phi_j - \Upsilon \delta\sigma_a \mathbf{s}_1 \cdot \Phi_j}{\sigma_a \mathbf{s}_1 \cdot \Phi_j}. \quad (70)$$

By taking linearization over the bilinear form (13), for any test function $\Psi \in [H^1(\Omega)]^{(N+1)/2}$,

$$B(\delta\Phi_j, \Psi) = - \int_{\Omega} [\delta\sigma_a (\mathbf{s}_1 \cdot \Phi_j) \mathbf{s}_1] \cdot \Psi dx. \quad (71)$$

Take $\Psi = \delta\Phi_j$, we can easily conclude that the following estimates from the coerciveness of $B(\cdot, \cdot)$:

$$\begin{aligned} \|\delta\Phi_j\|_{[H^1(\Omega)]^{(N+1)/2}} &= \mathcal{O} \left(N^{11/8} \|\delta\sigma_a (\mathbf{s}_1 \cdot \Phi_j)\|_{L^2(\Omega)} \|\mathbf{s}_1\|_{\ell^2} \right) \\ &= \mathcal{O} \left(N^{11/8} (1 + \log N) \|\delta\sigma_a (\mathbf{s}_1 \cdot \Phi_j)\|_{L^2(\Omega)} \right), \end{aligned} \quad (72)$$

On the other hand, multiply (68) with $s_{1,n}$ and sum over n ,

$$\delta\sigma_a \kappa_N (\mathbf{s}_1 \cdot \Phi_j) = -\nabla \cdot \left(\frac{1}{\sigma_s} \nabla (\mathbf{s}_1 \cdot \delta\Phi_j) \right) + \sigma_a \kappa_N \mathbf{s}_1 \cdot \delta\Phi_j + \sigma_s \mathbf{s}_1 \cdot \mathbf{Q} \delta\Phi_j, \quad (73)$$

therefore we have a straightforward estimate

$$\|\delta\sigma_a (\mathbf{s}_1 \cdot \Phi_j)\|_{L^2(\Omega)} = \mathcal{O} \left(\frac{\max(\kappa_N \|\mathbf{s}_1\|_{\ell^2}, \|\mathbf{s}_1 \cdot \mathbf{Q}\|_{\ell^2})}{\kappa_N} \|\delta\Phi_j\|_{[H^2(\Omega)]^{(N+1)/2}} \right), \quad (74)$$

where the constant $\kappa_N = \sum_{n=1}^{(N+1)/2} (4n-1)(1-g^{2n-1})s_{1,n}^2 = \Theta(N)$ and $\|\mathbf{s}_1 \cdot \mathbf{Q}\|_{\ell^2} \leq \mathcal{O}(N^2)$ from Lemma A.4. These two estimates imply that

$$c^{-1} N^{-11/8} (1 + \log N)^{-1} \|\delta\Phi_j\|_{[H^1(\Omega)]^{(N+1)/2}} \leq \|\delta\sigma_a (\mathbf{s}_1 \cdot \Phi_j)\|_{L^2(\Omega)} \leq cN \|\delta\Phi_j\|_{[H^2(\Omega)]^{(N+1)/2}}. \quad (75)$$

for some constant $c > 1$ independent of N .

Therefore if there exists two source distinct functions f_i, f_j such that the linear mapping $\delta\sigma_a \mapsto \mathcal{H}_{ij}$ is invertible and $\mathbf{s}_1 \cdot \Phi_j \neq 0$ over Ω , then one can recover both $\delta\sigma_a$ and $\delta\Phi_j$ from \mathcal{H}_{ij}

uniquely. In general such problem is ill-posed due to the compactness of the mapping $\delta\sigma_a \mapsto \mathcal{H}_{ij}$, numerical reconstruction of $\delta\sigma_a$ can be done through the following minimization formulation with regularization,

$$\delta\sigma_a^* = \arg \min_{\delta\sigma_a} \sum_{1 \leq i < j \leq J} \left[\left\| \mathcal{H}_{ij} - [(\mathbf{s}_1 \cdot \Phi_i)(\mathbf{s}_1 \cdot \delta\Phi_j) - (\mathbf{s}_1 \cdot \Phi_j)(\mathbf{s}_1 \cdot \delta\Phi_i)] \right\|_{L^2(\Omega)}^2 \right] + \alpha \left\| \nabla \delta\sigma_a \right\|_{L^2(\Omega)}^2,$$

where α is the regularization parameter.

Particularly, when the background absorption coefficient $\sigma_a = 0$ or negligible, then we approximately have $\delta H_i = \delta\sigma_a \Upsilon \mathbf{s}_1 \cdot \Phi_i$, which does not contain the perturbation $\delta\Upsilon$, in this case, we can only reconstruct $\delta\sigma_a$, the stability estimate is similar to the Theorem 3.1.

Without linearization, we take the ratio of two data sets H_i and H_j , then

$$\frac{H_i}{H_j} = \frac{\mathbf{s}_1 \cdot \Phi_i}{\mathbf{s}_1 \cdot \Phi_j}, \quad (76)$$

which only depends on σ_a , therefore our reconstruction strategy is similar to the linearized case. First, try to solve the minimization problem:

$$\sigma_a^* = \arg \min_{\sigma_a} \sum_{1 \leq i < j \leq J} \|H_i(\mathbf{s}_1 \cdot \Phi_j) - H_j(\mathbf{s}_1 \cdot \Phi_i)\|_{L^2(\Omega)}^2 + \alpha \|\nabla \sigma_a\|_{L^2(\Omega)}^2. \quad (77)$$

Then compute $\Upsilon^* = \frac{1}{J} \sum_{1 \leq i \leq J} \frac{H_i}{\sigma_a^* \mathbf{s}_1 \cdot \Phi_i}$ with the reconstructed σ_a^* .

Reconstruction of σ_s and σ_a . We consider the simultaneous reconstruction of both σ_s and σ_a from multiple sources f_j , $1 \leq j \leq J$ provided that Υ is known. Similar to the previous case, we denote H_j the measurement for f_j from the qPAT experiments. Under the linearized setting, let σ_a and σ_s the background absorption and scattering coefficients, the corresponding perturbations are $\delta\sigma_a$ and $\delta\sigma_s$. For each source f_j , let Φ_j the background solution and the perturbation in the solution is $\delta\Phi_j$, the corresponding perturbation in the measurement is δH_j . Linearize the variational form (20), we obtain the following equation,

$$\tilde{B}(\delta\Phi_j, \Psi) = - \int_{\Omega} \frac{\delta H_j}{\Upsilon} (\mathbf{s}_1 \cdot \Psi) d\mathbf{x} + \sum_{n=1}^{(N+1)/2} \int_{\Omega} \frac{\delta\sigma_s}{(4n-1)(1-g^{2n-1})} \left[\frac{1}{\sigma_s^2} \nabla \varphi_{1,n} \cdot \nabla \psi_n - \mathbf{q}_n \cdot \Phi_j \psi_n \right] d\mathbf{x},$$

where the bilinear form $\tilde{B}(\cdot, \cdot)$ is from (23) and \mathbf{q}_n is defined in (43). Hence the perturbation $\delta\Phi_j$ only linearly depends on $\delta\sigma_s$. On the other hand, since $\delta H_j / \Upsilon = \delta\sigma_a \mathbf{s}_1 \cdot \Phi_j + \sigma_a \mathbf{s}_1 \cdot \delta\Phi_j$, the crossing quantity $\mathcal{H}_{ij} = \frac{1}{\sigma_a \Upsilon^2} (H_i \delta H_j - H_j \delta H_i) = (\mathbf{s}_1 \cdot \Phi_i)(\mathbf{s}_1 \cdot \delta\Phi_j) - (\mathbf{s}_1 \cdot \Phi_j)(\mathbf{s}_1 \cdot \delta\Phi_i)$ only linearly depends on $\delta\sigma_s$, therefore we first try to reconstruct $\delta\sigma_s$ from \mathcal{H}_{ij} , then find $\delta\Phi_j$ and recover $\delta\sigma_a$ using

$$\delta\sigma_a = \frac{1}{J} \sum_{j=1}^J \left[\left(\frac{\delta H_j}{\Upsilon} - \sigma_a \mathbf{s}_1 \cdot \delta\Phi_j \right) / (\mathbf{s}_1 \cdot \Phi_j) \right]. \quad (78)$$

Similar to the previous case, the uniqueness is immediate if the crossing term \mathcal{H}_{ij} as a linear functional of $\delta\sigma_s$ is uniquely solvable and $\mathbf{s}_1 \cdot \Phi_j \neq 0$ over Ω . However since $\delta\sigma_s \mapsto \delta\Phi_j$ is a compact mapping, the inverse problem is ill-posed. Numerically, we consider the following L^2 optimization formulation with regularization:

$$\delta\sigma_s^* = \arg \min_{\delta\sigma_s} \sum_{1 \leq i < j \leq J} \left[\left\| \mathcal{H}_{ij} - [(\mathbf{s}_1 \cdot \Phi_i)(\mathbf{s}_1 \cdot \delta\Phi_j) - (\mathbf{s}_1 \cdot \Phi_j)(\mathbf{s}_1 \cdot \delta\Phi_i)] \right\|_{L^2(\Omega)}^2 \right] + \alpha \left\| \nabla \delta\sigma_s \right\|_{L^2(\Omega)}^2.$$

Additionally, if we are provided *a priori* estimate on the perturbation $\delta\sigma_a$ that $\|\frac{\delta\sigma_a H_i}{\Upsilon\sigma_a^2}\|_{H^2(\Omega)} \leq \varepsilon \ll 1$ for certain $1 \leq i \leq J$, then linearize the equation (55) for Φ_i , we obtain

$$-\nabla \cdot \left(\frac{-\delta\sigma_s}{\sigma_s^2} \nabla \mathbf{s}_1 \cdot \Phi_i \right) - \nabla \cdot \left(\frac{1}{\sigma_s} \nabla \mathbf{s}_1 \cdot \delta\Phi_i \right) + \kappa_N \frac{\delta H_i}{\Upsilon} + \mathbf{s}_1 \cdot (\delta\sigma_s \mathbf{Q}\Phi_i + \sigma_s \mathbf{Q}\delta\Phi_i) = 0, \quad (79)$$

where \mathbf{Q} is defined in (43) and $\kappa_N = \sum_{n=1}^{(N+1)/2} (4n-1)(1-g^{2n-1})s_{1,n}^2$. Following the similar approach in Theorem 3.7,

$$\begin{aligned} & \frac{1}{2} \int_{\Omega} \left(\frac{\delta\sigma_s}{\sigma_s} \right)^2 \left[\kappa_N \frac{H_i}{\Upsilon} (\mathbf{s}_1 \cdot \mathbf{Q}\Phi_i) + 3\sigma_s (\mathbf{s}_1 \cdot \mathbf{Q}\Phi_i)^2 - \frac{1}{\sigma_s} \nabla(\mathbf{s}_1 \cdot \Phi_i) \cdot \nabla(\mathbf{s}_1 \cdot \mathbf{Q}\Phi_i) \right] d\mathbf{x} \\ & = \int_{\Omega} \frac{\delta\sigma_s}{\sigma_s} \left[\nabla \cdot \left(\frac{1}{\sigma_s} \nabla \mathbf{s}_1 \cdot \delta\Phi_i \right) - \kappa_N \frac{\delta H_i}{\Upsilon} - \sigma_s (\mathbf{s}_1 \cdot \mathbf{Q}\delta\Phi_i) \right] (\mathbf{s}_1 \cdot \mathbf{Q}\Phi_i) d\mathbf{x}, \end{aligned} \quad (80)$$

Replace $\mathbf{s}_1 \cdot \delta\Phi_i = (\delta H_i - \delta\sigma_a H_i / \sigma_a) / (\Upsilon\sigma_a)$ and we immediately get the following estimate from the argument of Theorem 3.7 that

$$\begin{aligned} \int_{\Omega} \mathcal{V}_N(\mathbf{x}) \left(\frac{\delta\sigma_s}{\sigma_s} \right)^2 d\mathbf{x} & \leq C \left(N^2 \left\| \frac{\delta H_i}{\Upsilon\sigma_a} \right\|_{H^2(\Omega)}^2 + \left\| \frac{H_i \delta\sigma_a}{\Upsilon\sigma_a^2} \right\|_{H^2(\Omega)}^2 \right) \\ & \leq C \left(N^2 \left\| \frac{\delta H_i}{\Upsilon\sigma_a} \right\|_{H^2(\Omega)}^2 + \varepsilon^2 \right), \end{aligned} \quad (81)$$

where $\mathcal{V}_N(\mathbf{x})$ is the same as in the Theorem 3.7, C is a constant independent of N .

4 Numerical experiments

In this section, we perform our numerical experiments in two phases: (i). Assume the true model is certain SP_N system and then reconstruct the coefficients with exactly the same model; (ii). Assume the true model is either radiative transport equation or certain high order SP_N system, then the reconstruction is performed over a low order SP_N system.

In all the following numerical experiments, we use the unit square in 2D as our domain Ω . It is worthwhile to notice that all the previous arguments are meant for 3D only, the 2D experiments here should be interpreted as special cases (e.g. infinite tube) of 3D, assuming the solution is independent of the third dimension. The forward problem is solved though finite element method on a sufficiently fine mesh and the inverse problem is solved on a different mesh to avoid inverse crime. The source code for the numerical experiments is hosted on GitHub¹.

4.1 Experiment setting

In the following numerical experiments, we will use the boundary source functions $f_1(x, y) = 1 + x$, $f_2(x, y) = 1 + \sin(4\pi x)$ and the anisotropy constant $g = 0.8$. The coefficients $(\sigma_a, \sigma_s, \Upsilon)$ are selected from the following variable set, see Fig 2.

¹https://github.com/lowrank/spn_qpat

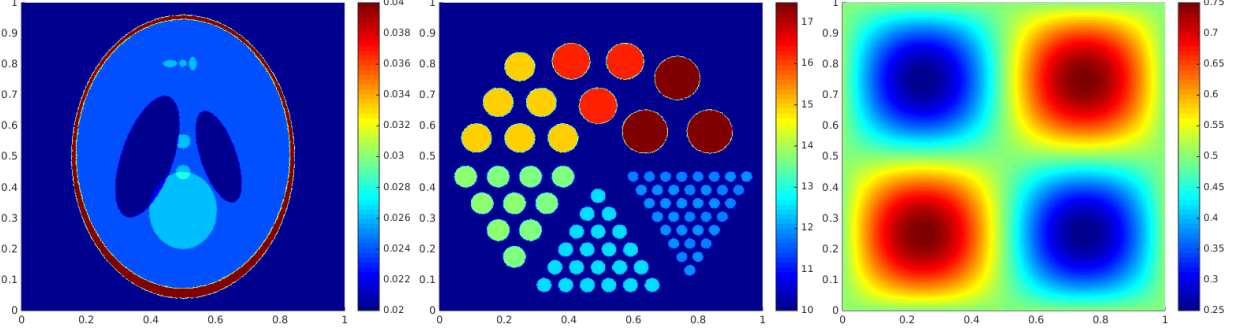


Figure 2: Coefficient Set. From left to right: absorption coefficient σ_a (Shepp-Logan phantom), scattering coefficient σ_s (Jaszczak phantom), Grüneisen coefficient Υ .

4.2 Validation of approximation

Before we start to run any of the numerical experiments, we need to verify that if our SP_N model is valid under these settings, which means modeling error should not be dominating (in practice there are noises in data). Therefore it is important to compare the quantity $\phi_0^N = \mathbf{s}_1 \cdot \Phi = \frac{H}{\sigma_a \Upsilon}$ with the solution's angular average $U(\mathbf{x}) = \int_{\mathbb{S}^{d-1}} u(\mathbf{x}, \mathbf{v}) d\mathbf{v}$ for the radiative transport equation (1). We summarize the L^2 relative errors: $\frac{\|\phi_0(\mathbf{x}) - U(\mathbf{x})\|}{\|U(\mathbf{x})\|}$ with respect to different SP_N models in Tab 1.

Table 1: Relative L^2 error of the ϕ_0^N from SP_N equations with the angular averaged solution $U(\mathbf{x})$ from radiative transport equation for boundary sources f_1 and f_2 .

	SP_1	SP_3	SP_5	SP_7	SP_9	SP_{11}	SP_{13}	SP_{15}	SP_{17}
f_1	1.93%	2.28%	2.25%	2.24%	2.23%	2.23%	2.23%	2.23%	2.23%
f_2	5.24%	3.98%	3.76%	3.75%	3.77%	3.78%	3.79%	3.79%	3.79%

From the table Tab 1, we can see that the modeling error with respect to the SP_N equations indeed stay at a relative low level with the selected coefficient set. The reason that such modeling error is not converging to zero might partly attribute to the simplification $\sigma_n \simeq (1 - g^n)\sigma_s$ in the computation instead of using $\sigma_a + (1 - g^n)\sigma_s$.

It is also informative to look at the convergence rate of ϕ_0^N from the SP_N equations with respect to growing N , see Fig 3. If the error converges sufficiently fast (e.g. exponentially), then we will obtain the uniqueness of reconstruction for the case that $N = \infty$. However, the theory about the convergence is still an open problem.

4.3 Reconstruction of σ_a only

In this numerical experiment, we are using the algorithm introduced in Section 3 to reconstruct the absorption coefficient σ_a only. We consider two scenarios for the reconstruction: (i) The datum H is generated from certain SP_N model. (ii) The datum H is generated from the radiative transport model. The result is summarized in the following Tab 2 and Tab 3. For all the reconstructions in the tables below, we have contaminated the datum H with multiplicative random noises pointwisely by $H^* = H(1 + \gamma \mathbf{random})$ with parameter $\gamma = 5\%$ regarded as the noise level and \mathbf{random} is the uniform distributed random variable on $[-1, 1]$.

Observe the diagonals of above tables, one can find out that the reconstruction error is not growing as N grows, this is because the estimate in Theorem 3.1 is only meant for the worst

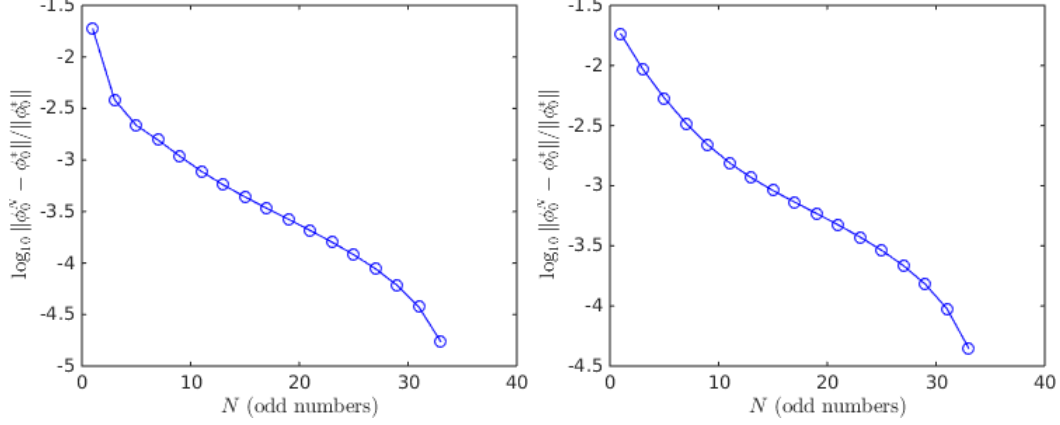


Figure 3: The convergence of ϕ_0^N with respect to the order N . Left: with source function f_1 . Right: with source function f_2 .

Table 2: Relative L^2 error of the reconstructed σ_a for source function f_1 with different generating models and reconstruction models. The row label represents the generating model and the column label represents the reconstruction model.

	SP_1	SP_3	SP_5	SP_7	SP_9	SP_{11}	SP_{13}	SP_{15}	SP_{17}
SP_1	2.89%	3.13%	3.15%	3.14%	3.14%	3.14%	3.14%	3.14%	3.14%
SP_3	3.08%	2.88%	2.88%	2.89%	2.89%	2.89%	2.89%	2.89%	2.89%
SP_5	3.13%	2.91%	2.91%	2.91%	2.91%	2.91%	2.91%	2.91%	2.91%
SP_7	3.09%	2.89%	2.88%	2.88%	2.88%	2.88%	2.88%	2.88%	2.88%
SP_9	3.06%	2.86%	2.86%	2.86%	2.86%	2.86%	2.86%	2.86%	2.86%
SP_{11}	3.07%	2.88%	2.88%	2.88%	2.88%	2.88%	2.88%	2.88%	2.88%
SP_{13}	3.11%	2.91%	2.91%	2.91%	2.91%	2.91%	2.91%	2.91%	2.91%
SP_{15}	3.09%	2.88%	2.88%	2.88%	2.88%	2.88%	2.88%	2.88%	2.88%
SP_{17}	3.10%	2.89%	2.89%	2.89%	2.89%	2.89%	2.89%	2.89%	2.89%
<i>RTE</i>	3.58%	3.14%	3.16%	3.18%	3.19%	3.19%	3.19%	3.19%	3.20%

boundary source. For the given source function and coefficient set, the reconstruction based on SP_1 model (diffusion approximation) appears not as good as the other models when the data are generated from SP_N models. While the performances of most low order SP_N models ($N \leq 7$) are already close to the ones of high order SP_N models ($N \geq 9$).

Particularly, when the datum H is generated from the radiative transport model, all of the reconstruction errors of SP_N models become larger due to the additional modeling errors, see Section 4.2. We plot some of the reconstructions in Fig 4. It is not surprising to find that the errors are relatively larger near boundary since the SP_N equation system is still elliptic over the whole domain, while the behavior of radiative transport averaged solution is hyperbolic in the vicinity of boundary sets.

Table 3: Same as Tab 2, but for source function f_2 .

	SP_1	SP_3	SP_5	SP_7	SP_9	SP_{11}	SP_{13}	SP_{15}	SP_{17}
SP_1	2.91%	3.17%	3.22%	3.22%	3.22%	3.22%	3.22%	3.22%	3.22%
SP_3	3.10%	2.88%	2.89%	2.90%	2.90%	2.90%	2.90%	2.90%	2.90%
SP_5	3.14%	2.89%	2.89%	2.89%	2.89%	2.89%	2.89%	2.89%	2.89%
SP_7	3.15%	2.89%	2.88%	2.88%	2.88%	2.88%	2.89%	2.89%	2.89%
SP_9	3.16%	2.91%	2.89%	2.89%	2.89%	2.89%	2.89%	2.89%	2.89%
SP_{11}	3.14%	2.89%	2.87%	2.87%	2.87%	2.87%	2.87%	2.87%	2.87%
SP_{13}	3.12%	2.88%	2.87%	2.87%	2.87%	2.87%	2.87%	2.87%	2.87%
SP_{15}	3.17%	2.91%	2.90%	2.89%	2.89%	2.89%	2.89%	2.89%	2.89%
SP_{17}	3.16%	2.90%	2.89%	2.89%	2.89%	2.89%	2.89%	2.89%	2.89%
RTE	8.02%	7.12%	6.77%	6.65%	6.60%	6.59%	6.60%	6.60%	6.61%

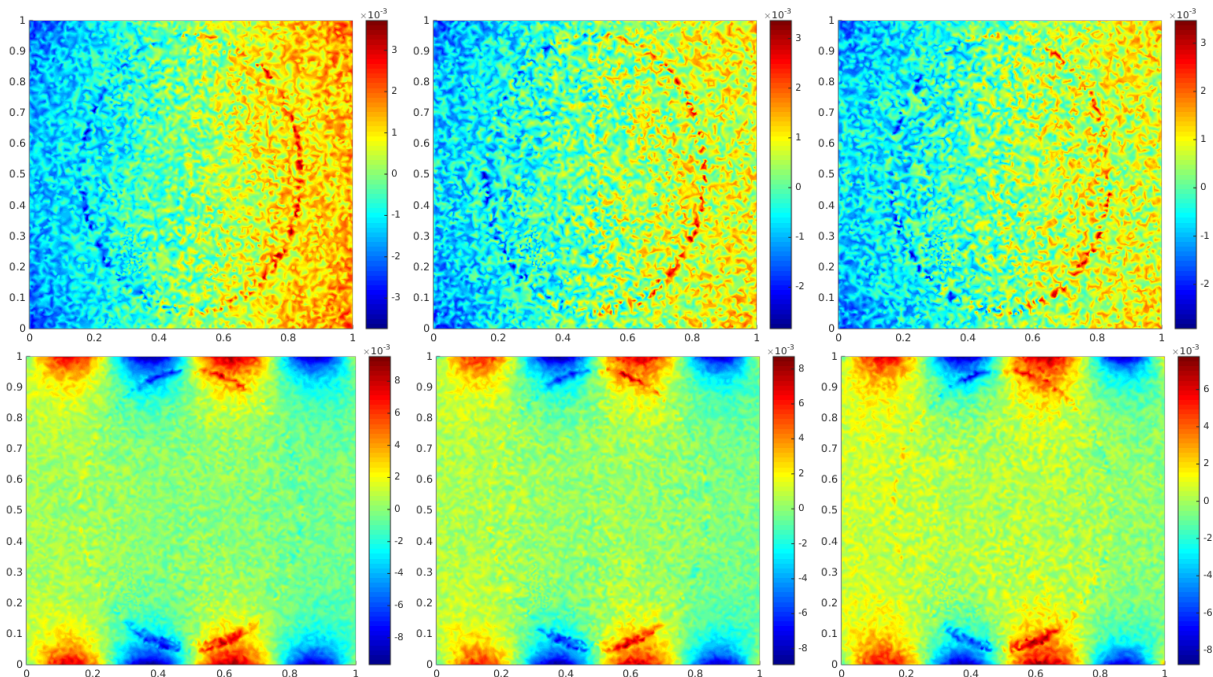


Figure 4: The error of reconstruction for the absorption coefficient σ_a with datum generated from radiative transport model. Top row, from left to right: reconstruction error for source f_1 with $N = 1$, $N = 7$, $N = 17$. Bottom row is the same but for source f_2 .

4.4 Reconstruction of σ_s only

The reconstruction of σ_s is a nonlinear problem for $N \geq 3$. In order to provide a fair comparison of across the SP_N models, we will use the optimization based method to reconstruct the scattering coefficient:

$$\sigma_s = \arg \min_{\sigma_s} \frac{1}{2} \int_{\Omega} (|H(\mathbf{x}) - H^*|^2 + |\nabla(H(\mathbf{x}) - H^*)|^2) d\mathbf{x} + \frac{\beta}{2} \int_{\Omega} |\nabla \sigma_s|^2 d\mathbf{x}, \quad (82)$$

where H^* is the measured datum and β is the regularization parameter. The optimization problem is solved by L-BFGS method, the gradient is computed from the adjoint state technique. The choice of regularization parameter β should depend on the noise level. One should notice that we use $H^1(\Omega)$ norm instead of the traditional $L^2(\Omega)$ minimization:

$$\sigma_s = \arg \min_{\sigma_s} \frac{1}{2} \int_{\Omega} |H(\mathbf{x}) - H^*|^2 d\mathbf{x} + \frac{\beta}{2} \int_{\Omega} |\nabla \sigma_s|^2 d\mathbf{x}. \quad (83)$$

This is due to the stability estimate in Theorem 3.7, where actually the $H^2(\Omega)$ norm is needed for the stability estimate. However, such regularity requirement implies that $H(\mathbf{x})$ needs to be globally C^1 from Sobolev embedding, which means our finite element space needs to equip with polynomials of five or higher degrees (e.g. Argyris element). Here we relax objective functional to $H^1(\Omega)$ norm simply to avoid the extraordinary computational cost. To get a brief impression about the two optimization schemes, we take the f_1 source function with SP_3 model (both data generation and reconstruction) for an example, the datum H is not contaminated (noise level $\gamma = 0$) and regularization parameter $\beta = 0$ as well. The reconstructed scattering coefficients are shown in Fig 5. One can tell from the images that the coefficient recovered from L^2 optimization (83) still contains background artifacts. The reason behind is the relatively strong smoothing effect of the mapping $\sigma_s(\mathbf{x}) \mapsto H(\mathbf{x})$, where the high frequency information in σ_s could not be fully recovered if we emphasize equally on $H(\mathbf{x})$'s frequency information.

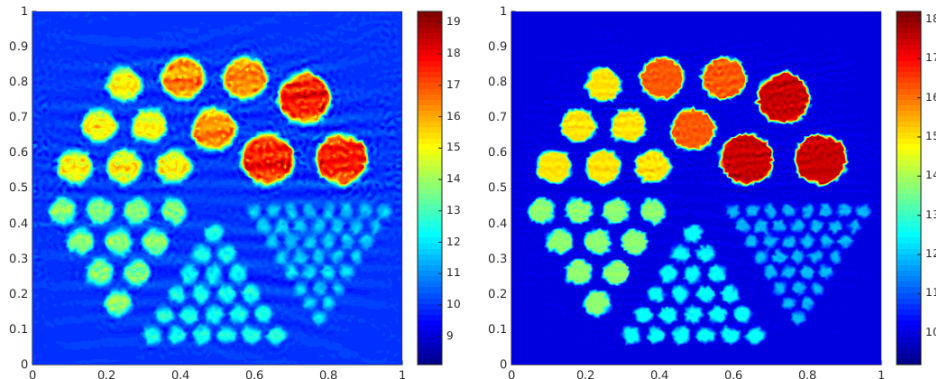


Figure 5: Left: The reconstructed scattering coefficient using L^2 minimization, the L^2 relative error is 4.25%. Right: The reconstructed scattering coefficient using H^1 minimization, the L^2 relative error is 1.10%.

Therefore the data contamination should be treated carefully for the H^1 minimization (82). This is because if we still apply the random noises by $H^* = H(1 + \gamma \mathbf{random})$ at each mesh node, then $\|H - H^*\|_{H^1(\Omega)} = \mathcal{O}(\sqrt{N}\gamma)$, where N is the total number of nodes assuming the mesh is uniform. Therefore instead of pointwise multiplicative noise, we aggressively contaminate the datum by perturbing its Fourier modes

$$\mathcal{F}H^*(\boldsymbol{\xi}) = \mathcal{F}H(\boldsymbol{\xi})(1 + \gamma \mathbf{random}), \quad (84)$$

where we have used $\gamma = 2\%$ as the noise level parameter. Note that such noise will perturb the low frequency modes of H which might cause severe global artifacts in the reconstruction.

Similar to the previous numerical experiment, we summarize the result in the Tab 4, where we have fixed the regularization parameter $\beta = 10^{-8}$ for these experiments. From the table, we could clearly see that SP_1 is not as good as other models for the reconstruction of σ_s when the datum H is coming from higher order models.

Table 4: Relative L^2 error of the reconstructed σ_s for source function f_1 with different generating models and reconstruction models. The row label represents the generating model and the column label represents the reconstruction model.

	SP_1	SP_3	SP_5	SP_7	SP_9	SP_{11}	SP_{13}	SP_{15}	SP_{17}
SP_1	12.0%	19.0%	19.5%	19.6%	19.6%	19.6%	19.6%	19.7%	19.7%
SP_3	13.9%	12.1%	12.5%	12.8%	13.0%	13.2%	13.3%	13.4%	13.5%
SP_5	14.9%	12.5%	12.3%	12.5%	12.7%	12.9%	13.0%	13.1%	13.2%
SP_7	15.1%	13.3%	12.5%	12.1%	11.9%	11.8%	11.7%	11.7%	11.6%
SP_9	15.1%	13.3%	12.5%	12.3%	12.2%	12.3%	12.3%	12.4%	12.4%
SP_{11}	15.5%	14.4%	13.3%	12.7%	12.3%	12.0%	11.8%	11.7%	11.6%
SP_{13}	15.1%	13.8%	12.8%	12.5%	12.3%	12.2%	12.2%	12.2%	12.2%
SP_{15}	15.7%	15.1%	14.0%	13.2%	12.7%	12.3%	12.1%	12.0%	11.8%
SP_{17}	15.2%	14.2%	13.1%	12.7%	12.4%	12.3%	12.2%	12.2%	12.2%
<i>RTE</i>	25.8%	25.7%	18.3%	21.5%	36.9%	37.2%	39.2%	39.3%	39.4%

Table 5: Same as Tab 4 but for source function f_2 .

	SP_1	SP_3	SP_5	SP_7	SP_9	SP_{11}	SP_{13}	SP_{15}	SP_{17}
SP_1	20.8%	21.4%	21.3%	23.1%	21.4%	21.4%	21.5%	21.6%	21.7%
SP_3	23.1%	18.0%	18.6%	19.1%	19.7%	19.9%	20.2%	20.3%	20.5%
SP_5	26.9%	18.3%	17.7%	18.0%	18.3%	18.5%	18.6%	18.6%	18.7%
SP_7	28.0%	22.7%	18.2%	16.4%	16.3%	16.4%	16.6%	16.8%	16.9%
SP_9	29.0%	19.9%	18.0%	17.8%	17.7%	17.8%	17.9%	18.06%	18.1%
SP_{11}	29.4%	19.5%	16.9%	16.4%	16.3%	16.3%	16.4%	16.4%	16.5%
SP_{13}	29.5%	21.0%	18.4%	18.0%	17.8%	17.8%	17.8%	17.8%	17.9%
SP_{15}	30.2%	20.6%	17.3%	16.6%	16.4%	16.3%	16.3%	16.3%	16.4%
SP_{17}	30.5%	21.5%	19.4%	18.1%	17.9%	17.8%	17.7%	17.8%	17.8%
<i>RTE</i>	55.9%	47.8%	49.4%	50.2%	50.3%	50.3%	51.4%	51.5%	51.6%

The reconstruction errors on the diagonal of the tables look converging as the order N grows, which indicates that the models converge relatively fast for the given source functions and the coefficient setting. When the datum H is generated from the radiative transport equation, the reconstruction error becomes larger. The reconstructions with respect to source function f_2 are significantly worse than the ones for f_1 , see Fig 6. However, this could be explained through the analogue with the SP_1 model, where the scattering coefficient's reconstruction is to solve a transport equation [5]:

$$\nabla\phi_0 \cdot \nabla D(x) + D(x)\Delta\phi_0 - \sigma_a\phi_0 = 0, \quad (85)$$

where $D(x) = 1/(3(1-g)\sigma_s)$, where ϕ_0 and $\sigma_s|_{\partial\Omega}$ are known. Therefore when $\nabla\phi_0 \neq 0$, the function $D(x)$ could be solved by tracing the characteristics. If $\nabla\phi_0$ vanishes or appears to be small, then the characteristics could be trapped, where the reconstructions are based on regularization only.

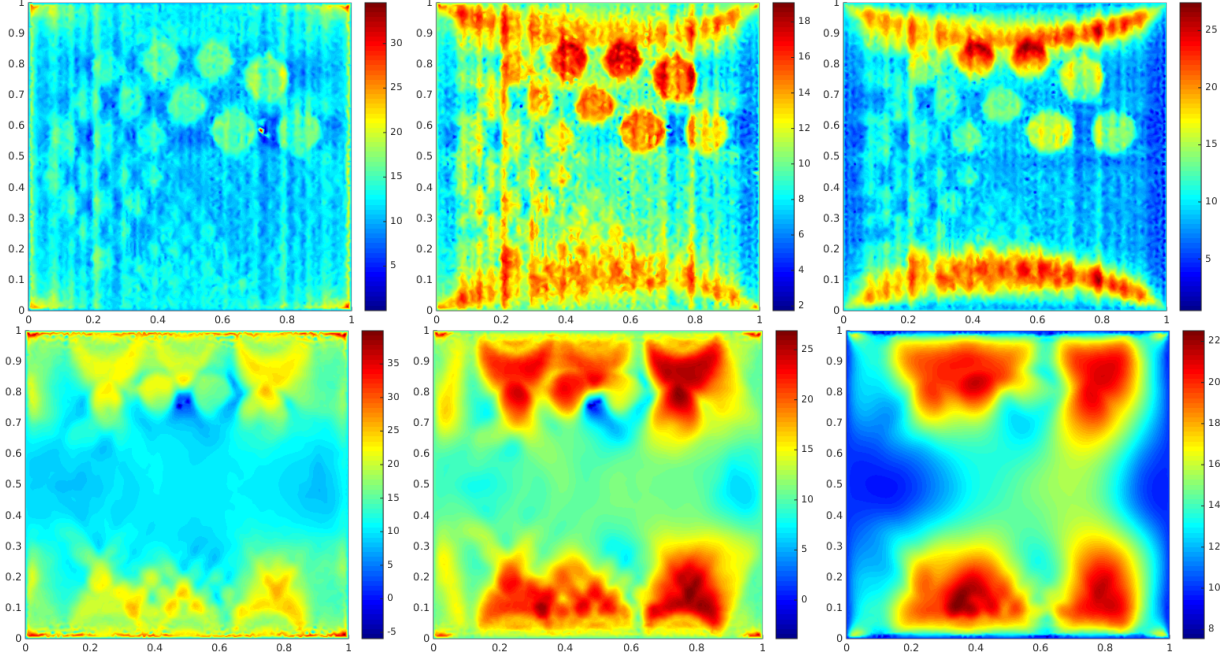


Figure 6: The reconstructions for the scattering coefficient σ_s with datum generated from radiative transport model. Top row, from left to right: reconstruction error for source f_1 with $N = 1, N = 7, N = 17$. Bottom row is the same but for source f_2 .

4.5 Reconstruction of σ_a and Υ

In this section, we consider the non-linearized case and follow the aforementioned two-step reconstruction strategy. Suppose H_1, H_2 are the data sets measured with boundary source functions f_1 and f_2 , respectively. Our numerical reconstruction solves the optimization problem:

$$\sigma_a^* = \arg \min_{\sigma_a} \left\| \frac{H_1}{H_2} - \frac{\mathbf{s}_1 \cdot \Phi_1}{\mathbf{s}_1 \cdot \Phi_2} \right\|_{L^2(\Omega)}^2 + \alpha \|\nabla \sigma_a\|_{L^2(\Omega)}^2, \quad (86)$$

where Φ_1, Φ_2 are the solutions to the SP_N equation with the absorption coefficient σ_a and source function f_1, f_2 , respectively. Intuitively, the ratio H_1/H_2 should be quite smooth and weakly depends on σ_a , which means the reconstruction for σ_a could be very unstable. In the following, we assume the data sets H_1 and H_2 are generated from the SP_N models with multiplicative noise $H_i^* = H_i(1 + \gamma \mathbf{random})$ for $\gamma = 0.1\%$ only, the regularization parameter is fixed as $\alpha = 10^{-8}$. Then we reconstruct the absorption coefficient using the same model. The reconstructions are shown in Fig 7, it could be seen that the reconstructions are very unstable even for small noise, only limited resolution could be obtained.

4.6 Reconstruction of σ_a and σ_s

Similar to the previous case, we consider the reconstruction in a two-step process as well. Suppose H_1, H_2 are the data sets with boundary sources f_1, f_2 , respectively. Our algorithm will first construct the scattering coefficient from the following optimization problem:

$$\sigma_s^* = \arg \min_{\sigma_s} \left\| \frac{H_1}{H_2} - \frac{\mathbf{s}_1 \cdot \Phi_1}{\mathbf{s}_1 \cdot \Phi_2} \right\|_{H^1(\Omega)}^2 + \alpha \|\nabla \sigma_s\|_{L^2(\Omega)}^2, \quad (87)$$

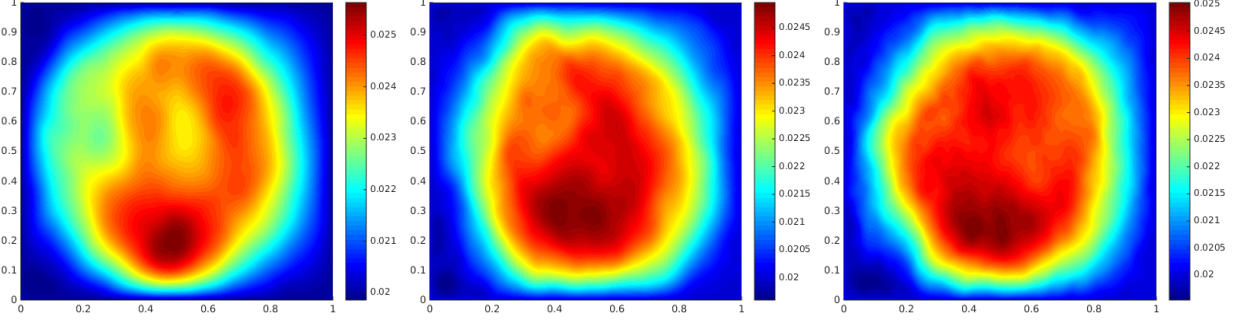


Figure 7: The reconstructions of absorption coefficients σ_a with respect to SP_N models. From left to right: $N = 1, 7, 17$. The relative L^2 errors are 16.6%, 16.2%, 15.9%, respectively.

where Φ_1, Φ_2 are the solutions to the modified SP_N equation (20), where σ_a has been replaced by $H_i/(\Upsilon \mathbf{s}_1 \cdot \Phi_i)$, $i = 1, 2$. Here we have taken the H_1 minimization. In the following numerical experiment, we assume H_1, H_2 are generated from the SP_N model, the data sets are contaminated on the Fourier space through

$$\mathcal{F}H_i^*(\boldsymbol{\xi}) = \mathcal{F}H_i(\boldsymbol{\xi})(1 + \gamma \text{random})$$

with $\gamma = 2\%$. We also fix the regularization parameter $\alpha = 10^{-8}$. The numerical reconstructions are performed over the same SP_N model and the results are illustrated in Fig 8. After the scattering coefficient has been reconstructed, we will use the recovered scattering coefficient to find the absorption coefficient following the Experiment 4.4. The corresponding reconstruction errors of the absorption coefficients are shown in Fig 9. It can be seen that even the reconstruction of scattering coefficients contain background artifacts, while the reconstruction errors of σ_a are still quite small.

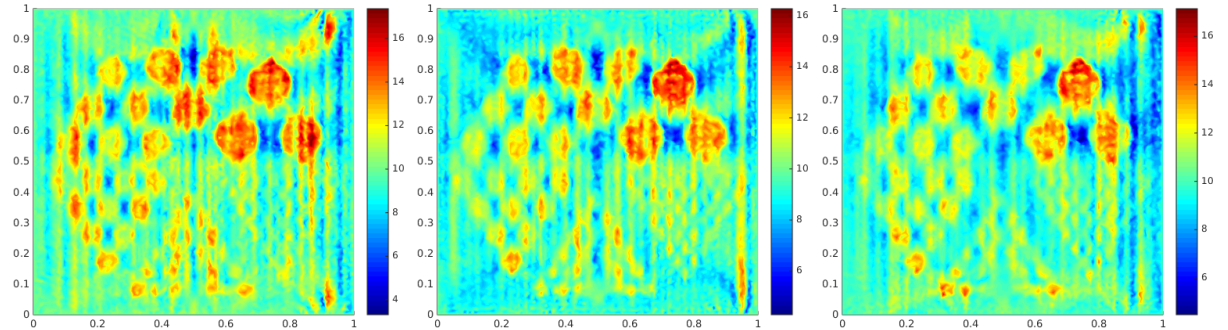


Figure 8: The reconstructions of scattering coefficients σ_s with respect to SP_N models. From left to right: $N = 1, 7, 17$. The relative L^2 errors are 16.1%, 16.7%, 16.8%, respectively.

5 Conclusion

In this work, we studied the quantitative photoacoustic tomography with the simplified P_N approximation model to the radiative transport equation. We have derived the uniqueness and stability estimates for the reconstruction of one single coefficient of $(\sigma_a, \sigma_s, \Upsilon)$ from one initial pressure datum $H(\mathbf{x})$. For the simultaneous reconstruction of two coefficients, we have considered the linearized setting and introduced the optimization based numerical algorithm for the reconstruction.

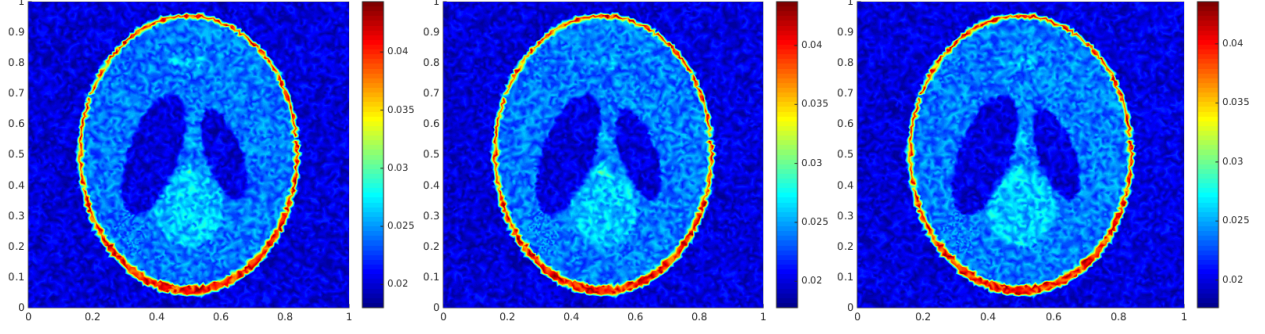


Figure 9: The reconstruction error of absorption coefficients σ_a with respect to SP_N models by using the recovered scattering coefficients from Fig 8. From left to right: $N = 1, 7, 17$. The relative L^2 errors are 1.76%, 5.79%, 5.80%, respectively.

We showed the numerical simulations based on a synthetic data to validate the mathematical analysis.

Acknowledgment

H. Zhao's research is partially supported by NSF DMS-2048877 and DMS-2012860.

A Appendix

Lemma A.1. Let $s_{k,l}$ be the (k,l) -th entry of M^{-1} , then

$$s_{k,l} = \begin{cases} \frac{1}{2k-1} (-1)^{l-k} \frac{((2l-2))!!}{(2l-1)!!} \frac{(2k-1)!!}{(2k-2)!!}, & l \geq k, \\ 0, & \text{otherwise.} \end{cases} \quad (88)$$

Proof. Let S be the matrix with (k,l) -th entry as $s_{k,l}$, we then compute the (k,j) -th entry of SM by $a_{k,j} := s_{k,j}(2j-1) + s_{k,j-1}(2j-2)$. If $k = j$, $s_{k,j} = \frac{1}{2j-1}$, therefore $a_{k,j} = \frac{1}{2j-1}(2j-1) = 1$. If $j < k$, notice that now $s_{k,j} = 0$, we must have $a_{k,j} = 0$. If $j > k$, we compute $a_{k,j}$ directly

$$\frac{1}{2k-1} \frac{(2k-1)!!}{(2k-2)!!} \left((-1)^{j-k} \frac{((2j-2))!!}{(2j-1)!!} (2j-1) + (-1)^{j-k-1} \frac{((2j-4))!!}{(2j-3)!!} (2j-2) \right) = 0. \quad (89)$$

Hence $S = M^{-1}$. □

Lemma A.2. $\det(R^{-1}) \leq \mathcal{O}(N^{3/8})$, hence $\det(R) \geq \mathcal{O}(N^{-3/8})$.

Proof. Since

$$\begin{aligned} R_{ij} &= (-1)^{i+j-1} \frac{2\Gamma(i+\frac{1}{2})\Gamma(j-\frac{1}{2})}{\pi\Gamma(i)\Gamma(j)} \frac{(4j-3)}{(2i+2j-2)(2j-2i-1)}, \\ &= (-1)^{i+j} \frac{\Gamma(i+\frac{1}{2})\Gamma(j-\frac{1}{2})}{\pi\Gamma(i)\Gamma(j)} \frac{2j-\frac{3}{2}}{(i-\frac{1}{4})^2 - (j-\frac{3}{4})^2}, \end{aligned} \quad (90)$$

which gives the factorization

$$R = UGV, \quad (91)$$

where diagonal matrices

$$\begin{aligned} U &= \text{diag}(u_1, \dots, u_{(N+1)/2}), \\ V &= \text{diag}(v_1, \dots, v_{(N+1)/2}), \end{aligned} \quad (92)$$

with $u_i = (-1)^i \sqrt{\frac{2}{\pi}} \frac{\Gamma(i+\frac{1}{2})}{\Gamma(i)}$, $v_j = (-1)^j \sqrt{\frac{2}{\pi}} \frac{\Gamma(j-\frac{1}{2})}{\Gamma(j)} (j - \frac{3}{4})$, and G is the Cauchy-Toeplitz matrix,

$$G = \left(\frac{1}{(i - \frac{1}{4})^2 - (j - \frac{3}{4})^2} \right)_{i,j=1,\dots,(N+1)/2}. \quad (93)$$

We denote $x_i = (i - \frac{1}{4})^2$ and $y_j = (j - \frac{3}{4})^2$, then use the Theorem 2.1 in [29],

$$G^{-1} = PG^TQ, \quad (94)$$

where $P = \text{diag}(p_1, \dots, p_{(N+1)/2})$ and $Q = \text{diag}(q_1, \dots, q_{(N+1)/2})$ satisfy

$$\begin{aligned} G[p_1, \dots, p_{(N+1)/2}]^T &= [1, \dots, 1]^T, \\ G^T[q_1, \dots, q_{(N+1)/2}]^T &= [1, \dots, 1]^T. \end{aligned} \quad (95)$$

Also p_i, q_j are computed explicitly by Cramer's law,

$$\begin{aligned} p_i &= \prod_{l=1, l \neq i}^{(N+1)/2} (x_l - y_i) / \prod_{l=1, l \neq i}^{(N+1)/2} (y_l - y_i), \\ q_j &= \prod_{l=1}^{(N+1)/2} (x_j - y_l) / \prod_{l=1, l \neq j}^{(N+1)/2} (x_j - x_l). \end{aligned} \quad (96)$$

By replacing x_i, y_j with their values, we obtain

$$\begin{aligned} p_i &= \prod_{l=1}^{(N+1)/2} (l+i-1)(l-i+\frac{1}{2}) / \prod_{l=1, l \neq i}^{(N+1)/2} (l-i)(l+i-3/2) \\ &= \left(\prod_{l=1}^{(N+1)/2} \frac{l+i-1}{l+i-\frac{3}{2}} \right) \left(\frac{1}{2} \prod_{l=1}^{i-1} \left(1 - \frac{1}{2l}\right) \prod_{l=1}^{(N+1)/2-i} \left(1 + \frac{1}{2l}\right) \right) \\ &= \frac{\Gamma(i + \frac{N+1}{2}) \Gamma(i - \frac{1}{2})}{\Gamma(i + \frac{N}{2}) \Gamma(i)} \left(2i - \frac{3}{2}\right) \left(\frac{1}{2} \prod_{l=1}^{i-1} \left(1 - \frac{1}{2l}\right) \prod_{l=1}^{(N+1)/2-i} \left(1 + \frac{1}{2l}\right) \right), \\ q_j &= \prod_{l=1}^{(N+1)/2} (j+l-1)(j-l+\frac{1}{2}) / \prod_{l=1, l \neq j}^{(N+1)/2} (j-l)(j+l-1/2) \\ &= \left(\prod_{l=1}^{(N+1)/2} \frac{j+l-1}{j+l-\frac{1}{2}} \right) \left(\frac{1}{2} \prod_{l=1}^{j-1} \left(1 + \frac{1}{2l}\right) \prod_{l=1}^{(N+1)/2-j} \left(1 - \frac{1}{2l}\right) \right) \\ &= \frac{\Gamma(j + \frac{N+1}{2}) \Gamma(j + \frac{1}{2})}{\Gamma(j + \frac{N}{2} + 1) \Gamma(j)} \left(2j - \frac{1}{2}\right) \left(\frac{1}{2} \prod_{l=1}^{j-1} \left(1 + \frac{1}{2l}\right) \prod_{l=1}^{(N+1)/2-j} \left(1 - \frac{1}{2l}\right) \right). \end{aligned} \quad (97)$$

Then we can easily deduce $\det(R^{-1}) = \sqrt{\det(P)\det(Q)/(\det(V)\det(U))}$, since all matrices involved are diagonal, let $S_i = \frac{\pi}{2} \prod_{l=1}^{i-1} (1 + \frac{1}{2l}) \prod_{l=1}^{(N+1)/2-i} (1 - \frac{1}{2l})$, then from the theory of Gamma functions, we know

$$S_i = \frac{\Gamma(i + \frac{1}{2})\Gamma(n - i + \frac{1}{2})}{\Gamma(i)\Gamma(\frac{(N+1)}{2} - i + 1)}. \quad (98)$$

Hence we can estimate $\det(R^{-1})$'s upper bound by estimating

$$\begin{aligned} \det(R^{-1}) &= \prod_{i=1}^{(N+1)/2} \frac{\sqrt{p_i q_i}}{u_i v_i} \\ &= \prod_{i=1}^{(N+1)/2} S_i \sqrt{\frac{\Gamma(i + \frac{N+1}{2})^2 \Gamma(i)^2 (i - \frac{1}{4})}{\Gamma(i + \frac{N}{2}) \Gamma(i + \frac{N}{2} + 1) \Gamma(i + \frac{1}{2}) \Gamma(i - \frac{1}{2}) (i - \frac{3}{4})}} \\ &= \prod_{i=1}^{(N+1)/2} \frac{\Gamma(i - \frac{1}{2})}{\Gamma(i)} \sqrt{\frac{\Gamma(i + \frac{(N+1)}{2})^2 (i - \frac{1}{2}) (i - \frac{1}{4})}{\Gamma(i + \frac{(N+1)}{2} - \frac{1}{2}) \Gamma(i + \frac{(N+1)}{2} + \frac{1}{2}) (i - \frac{3}{4})}}. \end{aligned} \quad (99)$$

Then by noticing the Chu's Double Inequality [7],

$$\sqrt{x - \frac{1}{4}} < \frac{\Gamma(x + \frac{1}{2})}{\Gamma(x)} < \frac{x}{\sqrt{x + \frac{1}{4}}}, \quad (100)$$

the following estimates hold,

$$\begin{aligned} \sqrt{\frac{\Gamma(i + \frac{N+1}{2})^2}{\Gamma(i + \frac{N}{2}) \Gamma(i + \frac{N}{2} + 1)}} &\leq \sqrt{\frac{i + \frac{(N+1)}{2} - \frac{1}{2}}{i + \frac{(N+1)}{2} - \frac{1}{4}}} < 1, \\ \sqrt{\frac{\Gamma(i - \frac{1}{2})^2 (i - \frac{1}{2}) (i - \frac{1}{4})}{\Gamma(i)^2 (i - \frac{3}{4})}} &\leq \sqrt{\frac{(i - \frac{1}{2}) (i - \frac{1}{4})}{(i - \frac{3}{4})^2}}, \end{aligned} \quad (101)$$

which implies

$$\begin{aligned} \det(R^{-1}) &< \prod_{i=1}^{(N+1)/2} \sqrt{\frac{(4i-2)(4i-1)}{(4i-3)^2}} \\ &= \exp\left(\frac{1}{2} \sum_{i=1}^{(N+1)/2} \log\left(1 + \frac{3}{4i-3} + \frac{2}{(4i-3)^2}\right)\right) \\ &\leq \exp\left(\frac{1}{2} \sum_{i=1}^{(N+1)/2} \frac{3}{4i-3} + \frac{2}{(4i-3)^2}\right) \\ &= \mathcal{O}\left(\exp\left(\frac{3}{8} \log\left(\frac{(N+1)}{2}\right)\right)\right) = \mathcal{O}(N^{3/8}). \end{aligned} \quad (102)$$

□

Lemma A.3. $\|R\|_F^2 \leq \frac{N+1}{2}$.

Proof. We show that for all $m \geq 1$,

$$\sum_{j=1}^m |R_{j,m}|^2 + \sum_{j=1}^{m-1} |R_{m,j}|^2 \leq 1. \quad (103)$$

The above estimate is true for $m = 1$ since $R_{1,1} = \frac{1}{2}$, we only focus on the cases that $m \geq 2$. Reformulate $R_{j,m}$ by the Gamma function as

$$|R_{j,m}| = \frac{\Gamma(j + \frac{1}{2})\Gamma(m - \frac{1}{2})}{\pi\Gamma(j)\Gamma(m)(j + m - 1)} \frac{(4m - 3)}{2m - 2j - 1}. \quad (104)$$

From the Chu's Double Inequality [7]

$$\sqrt{x - \frac{1}{4}} < \frac{\Gamma(x + \frac{1}{2})}{\Gamma(x)} < \frac{x}{\sqrt{x + \frac{1}{4}}}, \quad (105)$$

the following estimates hold,

$$\frac{\Gamma(j + \frac{1}{2})}{\Gamma(j)} < \frac{j}{\sqrt{j + \frac{1}{4}}}, \quad \frac{\Gamma(m - \frac{1}{2})}{\Gamma(m)} < \frac{1}{(m - \frac{3}{4})^{1/2}}, \quad (106)$$

we can deduce the estimate

$$\begin{aligned} \sum_{j=1}^m |R_{j,m}|^2 &= \frac{1}{\pi^2} \sum_{j=1}^m \left(\frac{\Gamma(j + \frac{1}{2})\Gamma(m - \frac{1}{2})}{\Gamma(j)\Gamma(m)} \right)^2 \frac{(4m - 3)^2}{(j + m - 1)^2} \frac{1}{(2m - 2j - 1)^2} \\ &\leq \frac{1}{\pi^2} \sum_{j=1}^m \frac{(4m - 3)^2 (j - \frac{1}{4} + \frac{1}{4(1+4j)})}{(m - \frac{3}{4})(j + m - 1)^2 (2m - 2j - 1)^2} \\ &\leq \frac{4}{\pi^2} \sum_{j=1}^m \frac{(4j - 1 + \frac{1}{(1+4j)})(4m - 3)}{(2j + 2m - 2)^2 (2m - 2j - 1)^2} \\ &= \frac{4}{\pi^2} \sum_{j=1}^m \left[\frac{1}{(2m - 2j - 1)^2} - \frac{1}{(2j + 2m - 2)^2} \right] \\ &\quad + \frac{4}{\pi^2} \sum_{j=1}^m \frac{(4m - 3)}{(1 + 4j)(2j + 2m - 2)^2 (2m - 2j - 1)^2} \\ &\leq \frac{4}{\pi^2} \left[\left(1 + \frac{\pi^2}{8} - \frac{1}{4m} \right) + \frac{1}{5m(2m - 3)^2} + \frac{1}{9m} \sum_{j=2}^m \frac{1}{(2m - 2j - 1)^2} \right] \\ &\leq \frac{4}{\pi^2} \left[\left(1 + \frac{\pi^2}{8} \right) + \left(\frac{11}{180} + \frac{\pi^2}{72} \right) \frac{1}{m} \right]. \end{aligned} \quad (107)$$

The other part can be estimated in a similar way,

$$\begin{aligned}
\sum_{j=1}^{m-1} |R_{m,j}|^2 &= \frac{1}{\pi^2} \sum_{j=1}^{m-1} \left(\frac{\Gamma(m + \frac{1}{2})\Gamma(j - \frac{1}{2})}{\Gamma(m)\Gamma(j)} \right)^2 \frac{(4j-3)^2}{(j+m-1)^2} \frac{1}{(2j-2m-1)^2} \\
&\leq \frac{1}{\pi^2} \sum_{j=1}^{m-1} \frac{(4j-3)^2(m - \frac{1}{4} + \frac{1}{4(1+4m)})}{(j - \frac{3}{4})(j+m-1)^2(2j-2m-1)^2} \\
&\leq \frac{4}{\pi^2} \sum_{j=1}^{m-1} \frac{(4m-1 + \frac{1}{1+4m})(4j-3)}{(2j+2m-2)^2(2j-2m-1)^2} \\
&= \frac{4}{\pi^2} \sum_{j=1}^{m-1} \left[\frac{1}{(2m+1-2j)^2} - \frac{1}{(2j+2m-2)^2} \right] \\
&\quad + \frac{4}{\pi^2} \sum_{j=1}^{m-1} \frac{4j-3}{(1+4m)(2j+2m-2)^2(2m+1-2j)^2} \\
&\leq \frac{4}{\pi^2} \left[\left(\frac{\pi^2}{8} - 1 - \frac{1}{4m} \right) + \sum_{j=1}^{m-1} \frac{1}{4m^2(2m+1-2j)^2} \right] \\
&\leq \frac{4}{\pi^2} \left[\left(\frac{\pi^2}{8} - 1 - \frac{1}{4m} \right) + \left(\frac{\pi^2}{8} - 1 \right) \frac{1}{4m^2} \right].
\end{aligned} \tag{108}$$

Hence we can estimate that

$$\sum_{j=1}^m |R_{j,m}|^2 + \sum_{j=1}^{m-1} |R_{m,j}|^2 \leq 1 - \frac{4}{\pi^2} \left(\frac{17}{90} - \frac{\pi^2}{72} \right) \frac{1}{m} + \frac{1}{\pi^2} \left(\frac{\pi^2}{8} - 1 \right) \frac{1}{m^2}, \tag{109}$$

the above estimate is strictly less than 1 for $m \geq 2$, then the Frobenius norm's square of R is estimated by

$$\|R\|_F^2 = \frac{1}{2} + \sum_{m=2}^{(N+1)/2} \left(\sum_{j=1}^m |R_{j,m}|^2 + \sum_{j=1}^{m-1} |R_{m,j}|^2 \right) \leq \frac{N}{2}. \tag{110}$$

□

Lemma A.4. Let \mathbf{s}_k the k -th row of the matrix T^{-1} in (7), and matrix \mathbf{Q} is defined in (43), then

$$\|\mathbf{s}_1 \cdot \mathbf{Q}\|_{\ell^p} = \mathcal{O}(N^{3/2+1/p}). \tag{111}$$

Proof. Let $s_{k,j}$ denote the j -th entry of vector \mathbf{s}_k . Combine the Lemma A.1 and Gautschi's inequality [12], we have

$$|s_{k,j}| < \frac{1}{2k-1} \frac{\sqrt{k + \frac{1}{2}}}{\sqrt{j - \frac{1}{2}}}. \tag{112}$$

For the matrix \mathbf{Q} , we denote its (n, j) -th entry by Q_{nj} , which can be estimated by

$$\begin{aligned}
|Q_{nj}| &\leq (4n-1) \sum_{k \geq 2}^{\min(j,n)} (4k-3) |s_{k,n} s_{k,j}| \leq (4n-1) \sum_{k \geq 2}^{\min(j,n)} \frac{(4k-3)}{(2k-1)^2} \frac{k + \frac{1}{2}}{\sqrt{j - \frac{1}{2}} \sqrt{n - \frac{1}{2}}} \\
&\leq \frac{(4n-1)}{\sqrt{j - \frac{1}{2}} \sqrt{n - \frac{1}{2}}} \sum_{k \geq 2}^{\min(j,n)} \frac{(4k-3)(k + \frac{1}{2})}{(2k-1)^2}.
\end{aligned} \tag{113}$$

Since $(4k - 3)(k + \frac{1}{2}) \leq 2(2k - 1)^2$ for all k , we will have $|Q_{n,j}| \leq \frac{(8n-2)}{\sqrt{n-\frac{1}{2}}\sqrt{j-\frac{1}{2}}}(\min(j, n) - 1)$, therefore, by simple calculations, $\|\mathbf{s}_1 \cdot \mathbf{Q}\|_{\ell^\infty}$ is bounded by

$$\begin{aligned} \|\mathbf{s}_1 \cdot \mathbf{Q}\|_{\ell^\infty} &\leq \sup_{j \geq 1} \sum_{n \geq 1} |s_{1,n}| |Q_{n,j}| \leq \sup_{j \geq 1} \sum_{n \geq 1} \frac{(8n - 2)(\min(j, n) - 1)}{(n - \frac{1}{2})\sqrt{j - \frac{1}{2}}} \\ &= \mathcal{O}(N^{3/2}). \end{aligned} \tag{114}$$

Then the ℓ^p estimate is

$$\|\mathbf{s}_1 \cdot \mathbf{Q}\|_{\ell^p} \leq \|\mathbf{s}_1 \cdot \mathbf{Q}\|_{\ell^\infty} \left(\frac{(N + 1)}{2} \right)^{1/p} = \mathcal{O}(N^{3/2+1/p}).$$

□

References

- [1] M. AGRANOVSKY, P. KUCHMENT, AND L. KUNYANSKY, *On reconstruction formulas and algorithms for the thermoacoustic and photoacoustic tomography*, Preprint, (2007).
- [2] H. AMMARI, E. BRETIN, V. JUGNON, AND A. WAHAB, *Photoacoustic imaging for attenuating acoustic media*, in *Mathematical modeling in biomedical imaging II*, Springer, 2012, pp. 57–84.
- [3] G. BAL, *Hybrid inverse problems and internal functionals*, *Inverse problems and applications: inside out. II*, 60 (2013), pp. 325–368.
- [4] G. BAL, A. JOLLIVET, AND V. JUGNON, *Inverse transport theory of photoacoustics*, *Inverse Problems*, 26 (2010), p. 025011.
- [5] G. BAL AND K. REN, *Multi-source quantitative photoacoustic tomography in a diffusive regime*, *Inverse Problems*, 27 (2011), p. 075003.
- [6] P. BEARD, *Biomedical photoacoustic imaging*, *Interface focus*, 1 (2011), pp. 602–631.
- [7] J. CHU, *A modified wallis product and some applications*, *The American Mathematical Monthly*, 69 (1962), pp. 402–404.
- [8] M. CHU, K. VISHWANATH, A. D. KLOSE, AND H. DEGHANI, *Light transport in biological tissue using three-dimensional frequency-domain simplified spherical harmonics equations*, *Physics in Medicine & Biology*, 54 (2009), p. 2493.
- [9] B. COX, J. LAUFER, AND P. BEARD, *The challenges for quantitative photoacoustic imaging*, in *Photons Plus Ultrasound: Imaging and Sensing 2009*, vol. 7177, International Society for Optics and Photonics, 2009, p. 717713.
- [10] T. DING, K. REN, AND S. VALLÉLIAN, *A one-step reconstruction algorithm for quantitative photoacoustic imaging*, *Inverse Problems*, 31 (2015), p. 095005.
- [11] C. FREDERICK, K. REN, AND S. VALLÉLIAN, *Image reconstruction in quantitative photoacoustic tomography with the simplified p_2 approximation*, *SIAM Journal on Imaging Sciences*, 11 (2018), pp. 2847–2876.

- [12] W. GAUTSCHI, *Some elementary inequalities relating to the gamma and incomplete gamma function*, J. Math. Phys, 38 (1959), pp. 77–81.
- [13] E. M. GELBARD, *Application of spherical harmonics method to reactor problems*, Bettis Atomic Power Laboratory, West Mifflin, PA, Technical Report No. WAPD-BT-20, (1960).
- [14] A. D. GÜNGÖR, *Erratum to “an upper bound for the condition number of a matrix in spectral norm”*[*j. comput. appl. math.* 143 (2002) 141–144], Journal of Computational and Applied Mathematics, 234 (2010), p. 316.
- [15] M. HALTMEIER, T. SCHUSTER, AND O. SCHERZER, *Filtered backprojection for thermoacoustic computed tomography in spherical geometry*, Mathematical methods in the applied sciences, 28 (2005), pp. 1919–1937.
- [16] Y. HRISTOVA, *Time reversal in thermoacoustic tomography—an error estimate*, Inverse Problems, 25 (2009), p. 055008.
- [17] A. D. KLOSE AND E. W. LARSEN, *Light transport in biological tissue based on the simplified spherical harmonics equations*, Journal of Computational Physics, 220 (2006), pp. 441–470.
- [18] ———, *Simplified spherical harmonics methods for modeling light transport in biological tissue*, in Biomedical Topical Meeting, Optical Society of America, 2006, p. MH3.
- [19] P. KUCHMENT AND L. KUNYANSKY, *Mathematics of thermoacoustic and photoacoustic tomography*, preprint, (2007).
- [20] A. V. MAMONOV AND K. REN, *Quantitative photoacoustic imaging in radiative transport regime*, arXiv preprint arXiv:1207.4664, (2012).
- [21] A. W. MARSHALL, I. OLKIN, AND B. C. ARNOLD, *Inequalities: theory of majorization and its applications*, vol. 143, Springer, 1979.
- [22] R. G. MCCLARREN, *Theoretical aspects of the simplified pn equations*, Transport Theory and Statistical Physics, 39 (2010), pp. 73–109.
- [23] W. MCLEAN AND W. C. H. MCLEAN, *Strongly elliptic systems and boundary integral equations*, Cambridge university press, 2000.
- [24] G. PIAZZA AND T. POLITI, *An upper bound for the condition number of a matrix in spectral norm*, Journal of Computational and Applied Mathematics, 143 (2002), pp. 141–144.
- [25] K. REN, H. GAO, AND H. ZHAO, *A hybrid reconstruction method for quantitative pat*, SIAM Journal on Imaging Sciences, 6 (2013), pp. 32–55.
- [26] O. SCHERZER, *Handbook of mathematical methods in imaging*, Springer Science & Business Media, 2010.
- [27] P. STEFANOV AND G. UHLMANN, *Thermoacoustic tomography with variable sound speed*, Inverse Problems, 25 (2009), p. 075011.
- [28] E. E. TYRTYSHNIKOV, *Cauchy-toeplitz matrices and some applications*, Linear Algebra and its Applications, 149 (1991), pp. 1–18.

- [29] ———, *Singular values of cauchy-toeplitz matrices*, Linear algebra and its applications, 161 (1992), pp. 99–116.
- [30] L. V. WANG, *Photoacoustic imaging and spectroscopy*, CRC press, 2017.
- [31] S. WRIGHT, M. SCHWEIGER, AND S. ARRIDGE, *Reconstruction in optical tomography using the pn approximations*, Measurement Science and Technology, 18 (2006), p. 79.
- [32] W. P. ZIEMER, *Weakly differentiable functions: Sobolev spaces and functions of bounded variation*, vol. 120, Springer Science & Business Media, 2012.